

Supplementary Information for:
Hidden partners: Using cross-docking calculations to predict binding sites for
proteins with multiple interactions

Nathalie Lagarde¹, Alessandra Carbone^{2,3} and Sophie Sacquin-Mora¹

¹ Laboratoire de Biochimie Théorique, CNRS UPR9080, Institut de Biologie Physico-Chimique, University Paris Diderot, Sorbonne Paris Cité, 13 rue Pierre et Marie Curie, 75005, Paris, France

² Laboratoire de Biologie Computationnelle et Quantitative, CNRS UMR7238, UPMC Univ-Paris 6, Sorbonne Université, 4 place Jussieu, 75005, Paris, France

³ Institut Universitaire de France, 75005, Paris, France

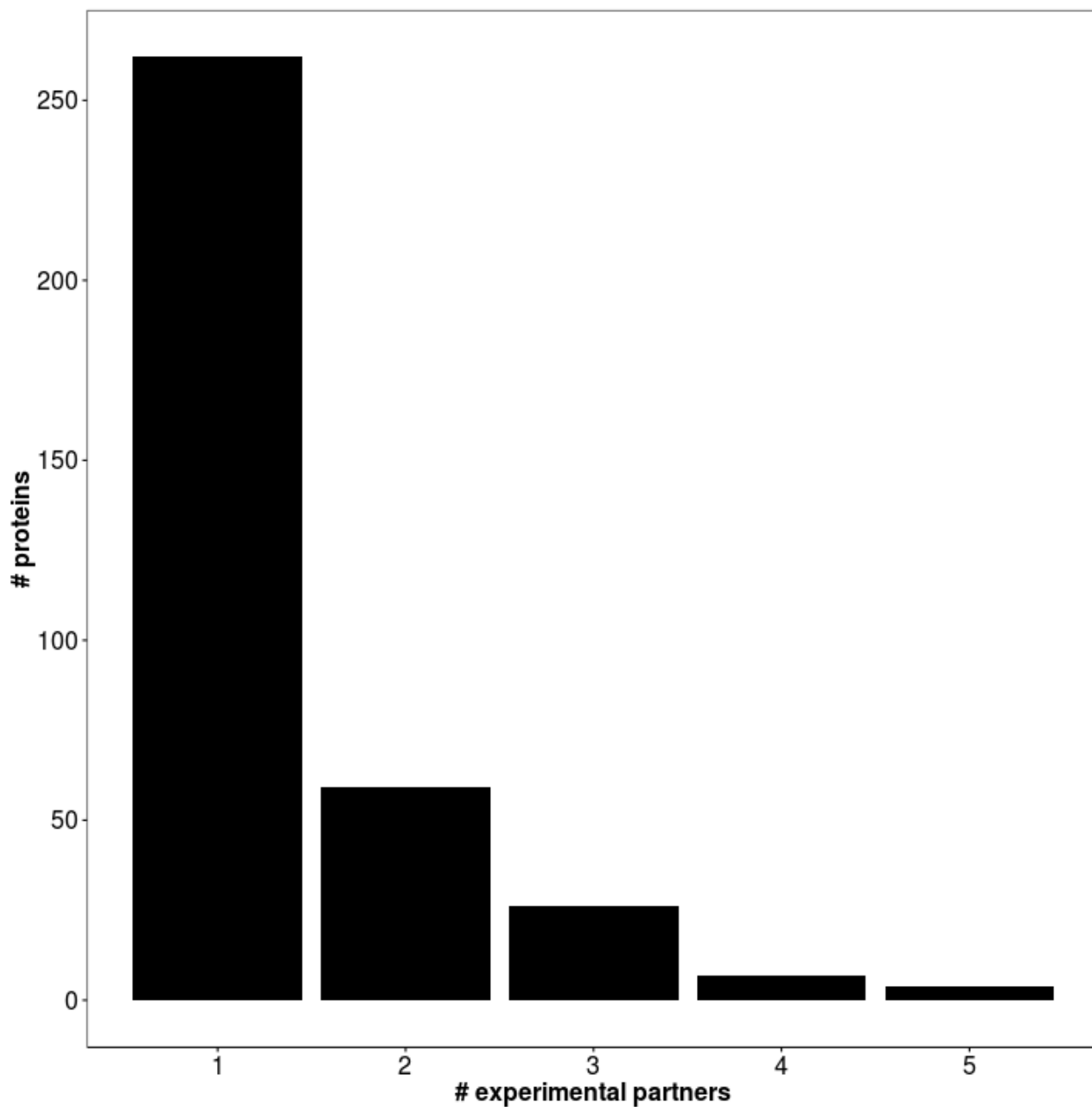
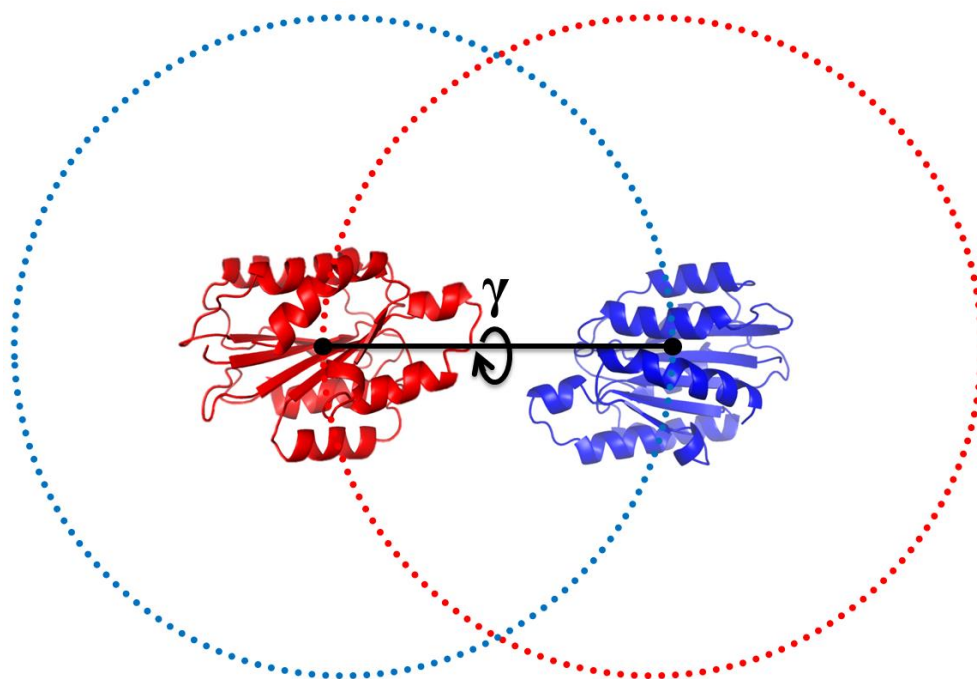
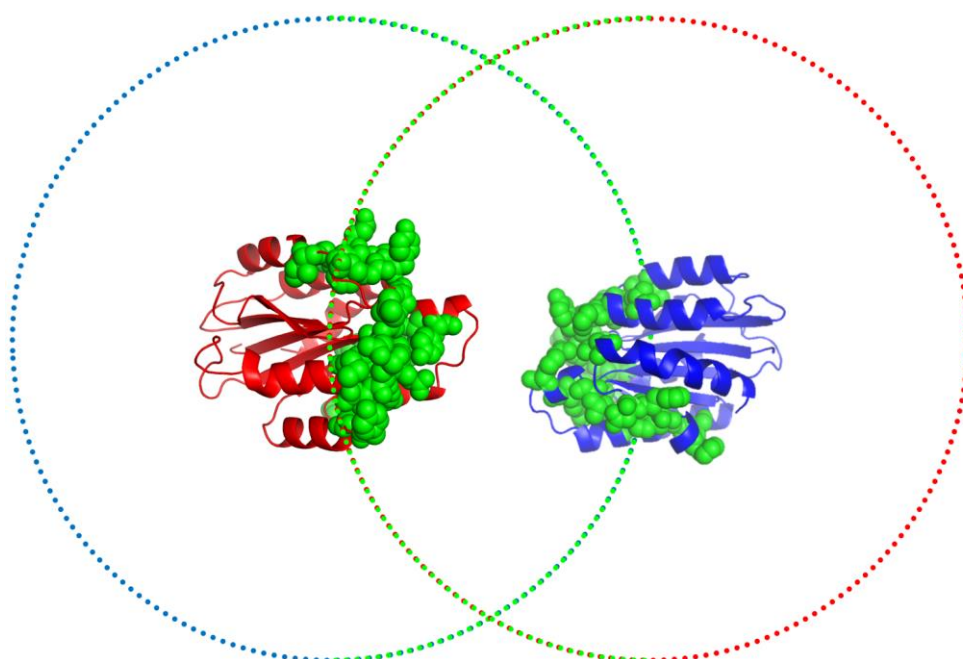


Figure S1 : Distribution of the number of experimental partners among the proteins included in our cross-docking dataset.



A

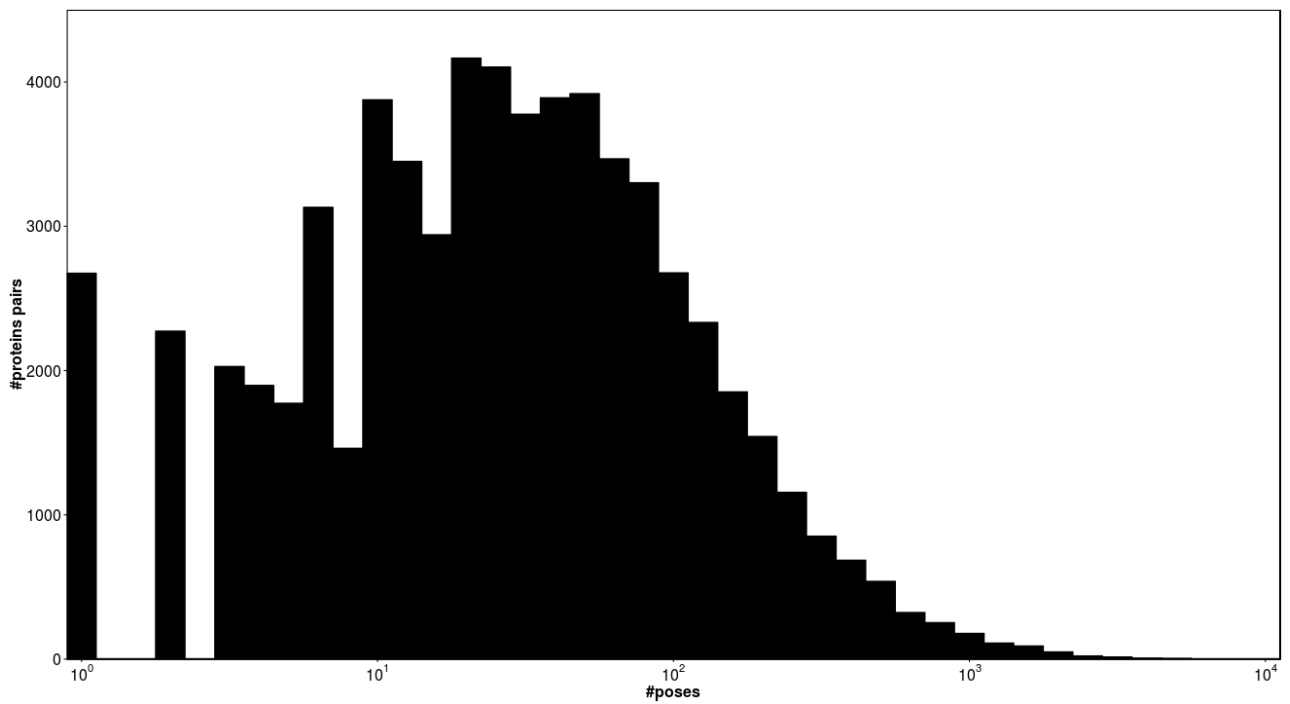


B

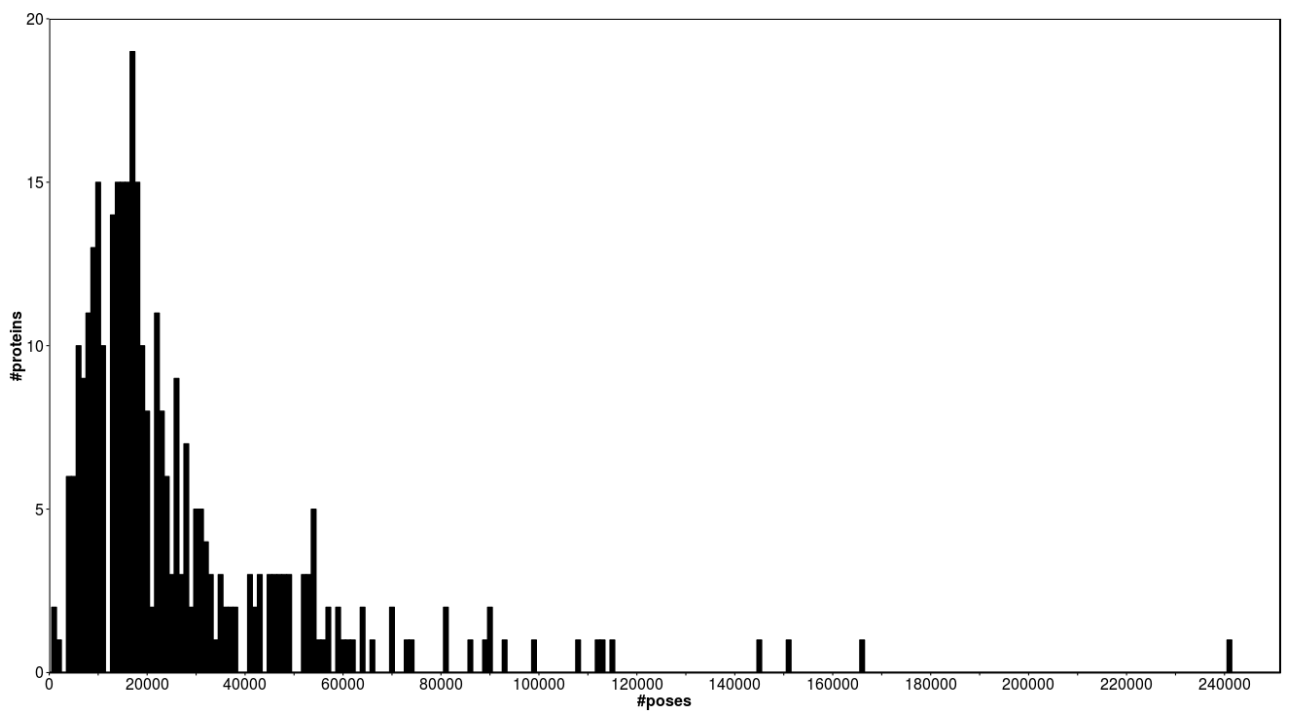
Figure S2: Starting orientations generation for the rat A1B1 integrin i-domain complex (PDB code 1CK4, 1CK4_A in red and 1CK4_B in blue). The systematically generated starting positions for the receptor and ligand proteins are plotted as blue and red points.

(A) Different starting orientations were generated for each starting positions of the receptor and ligand proteins by applying 5 rotations of the gamma Euler angle defined with the axis connecting the centers of mass of the 2 proteins.

(B) After filtration using JET information, docking calculations are only performed for those starting points that are located at the vicinity of JET predicted interface residues (plotted as green spheres on the proteins), thus considerably reducing the computation time.



A

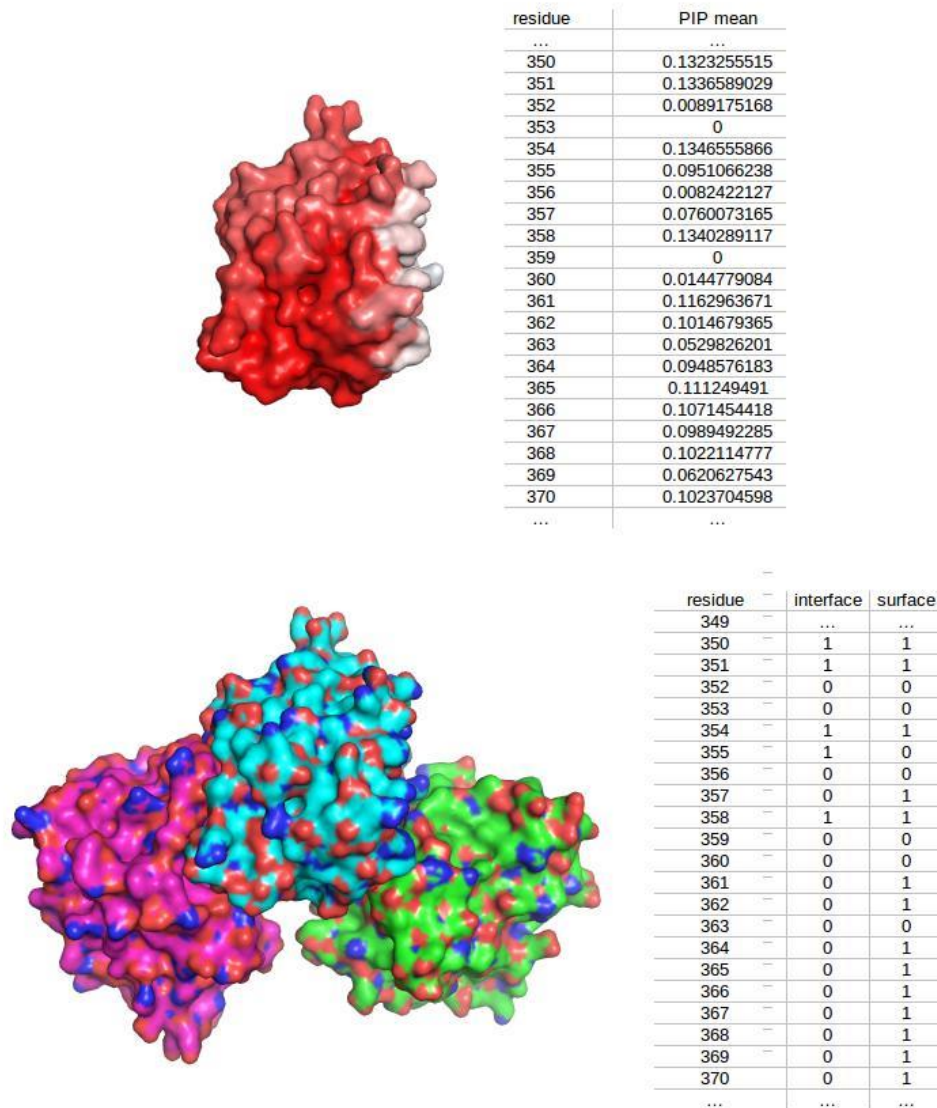


B

Figure S3 :

(A) Distribution of the number of kept docking poses (using a logarithmic scale) for each protein pair after filtering on the interaction energy.

(B) Final distribution of the number of kept docking poses for each protein (taking into account all its partners) after filtering on the interaction energy.



AUC=0.619

Figure S4(A): « Global interface » (GI) scoring scheme computed for the protein 1IW0_B (represented in cyan in the bottom panel) that presents 2 experimental partners: 1IW0_C and 1IW0_A (respectively in magenta and green in the bottom panel) . The GI score is computed by comparing the PIP values (mapped on the protein's surface in the top panel, high PIP residues showed in white and low PIP residues in red) with one single global reference experimental interface generated by concatenating all the existing experimental interfaces. If a residue is part of the experimental interface between the query protein and at least one of the partners, it is tagged as interface residue in the global reference experimental interface (1 in the « interface » column). Conversely, if a residue is not part of any experimental interfaces, it is tagged as non interface residue (0 in the « interface » column).

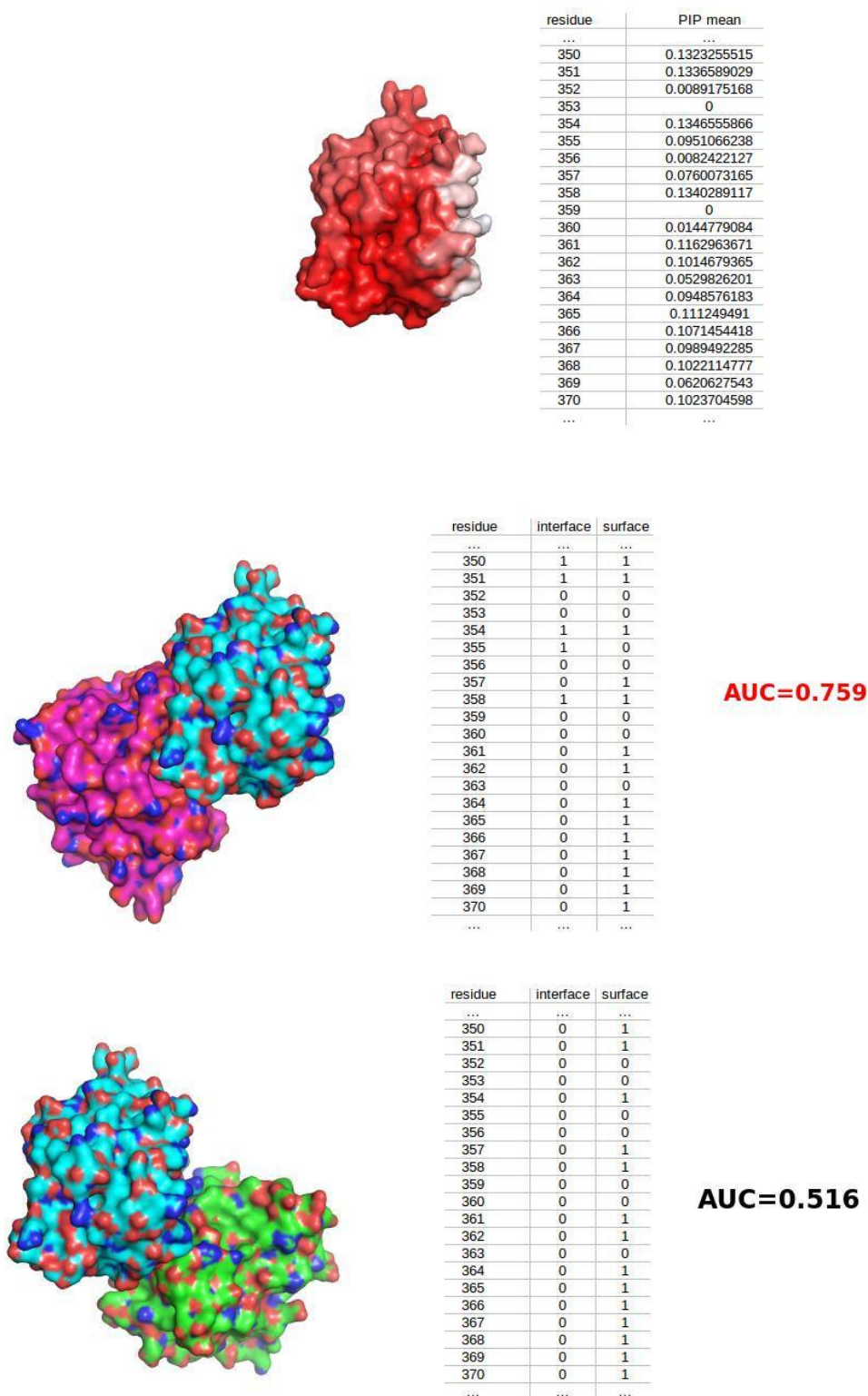


Figure S4(B): «Best interface» (BI) scoring scheme computed for the protein 1IW0_B (represented in cyan in the middle and bottom panels) that presents 2 experimental partners: 1IW0_C (in magenta in the middle panel) and 1IW0_A (in green in the bottom panel). The BI score is computed by comparing the PIP values (mapped on the protein's surface in the top panel, high PIP residues showed in blue and low PIP residues in red) to each reference experimental interface separately, and only the predicted interface associated with the best binding site prediction performance was kept.

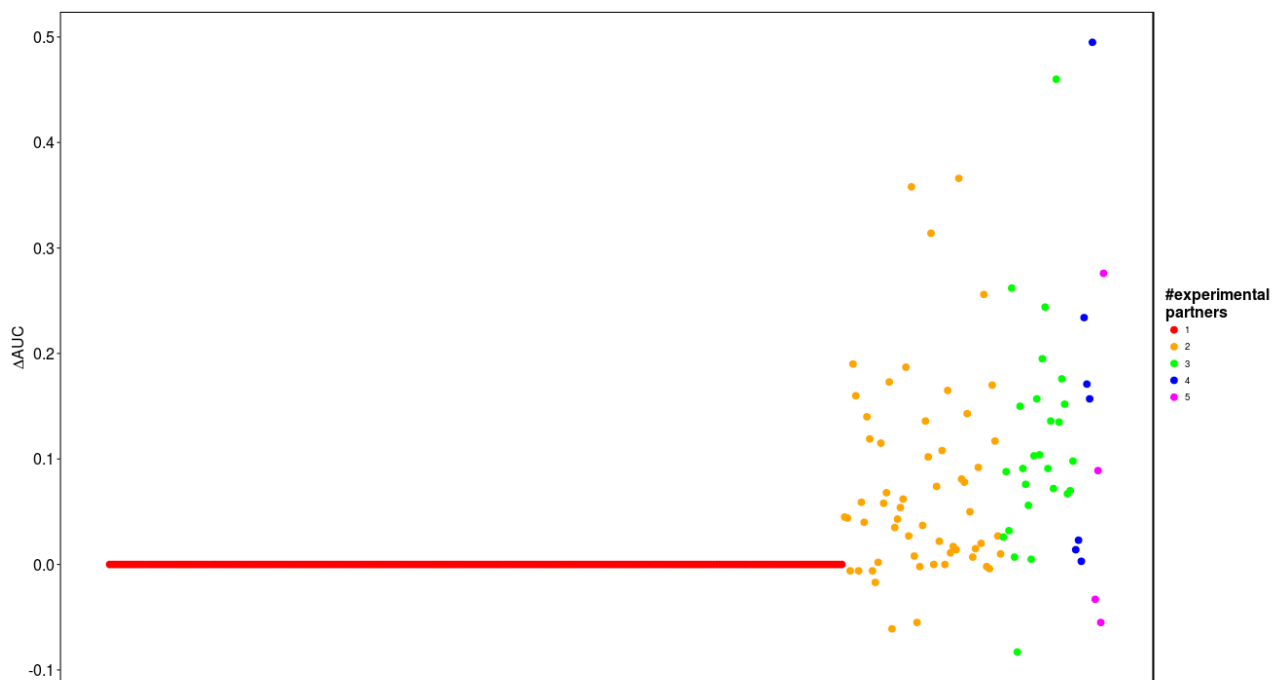


Figure S5 : Variation of AUC observed for each protein (the x-axis represents the proteins of the SubHCMD dataset ranked according to their number of partners) between the GI score and the BI score ($\Delta AUC = AUC_{BI} - AUC_{GI}$), the dots colors indicate the number of experimental partners included in the CC-D for each protein.

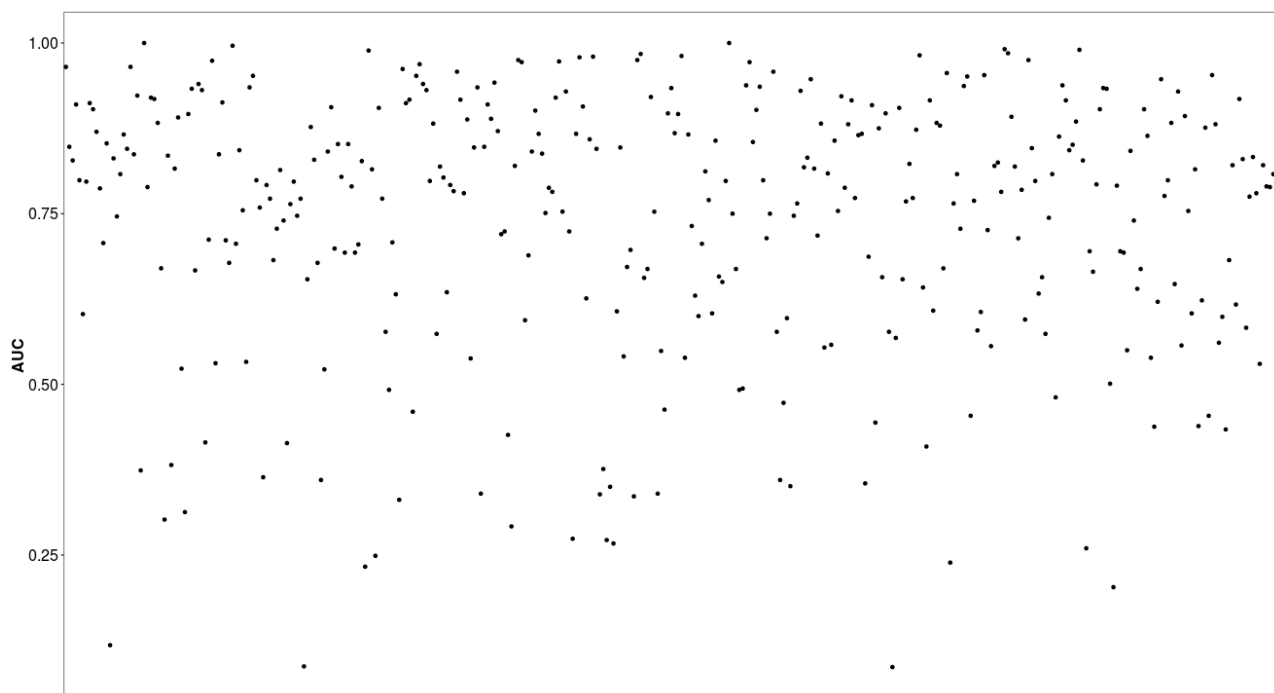


Figure S6 : AUC value for each protein in our CC-D dataset obtained with the BI score.

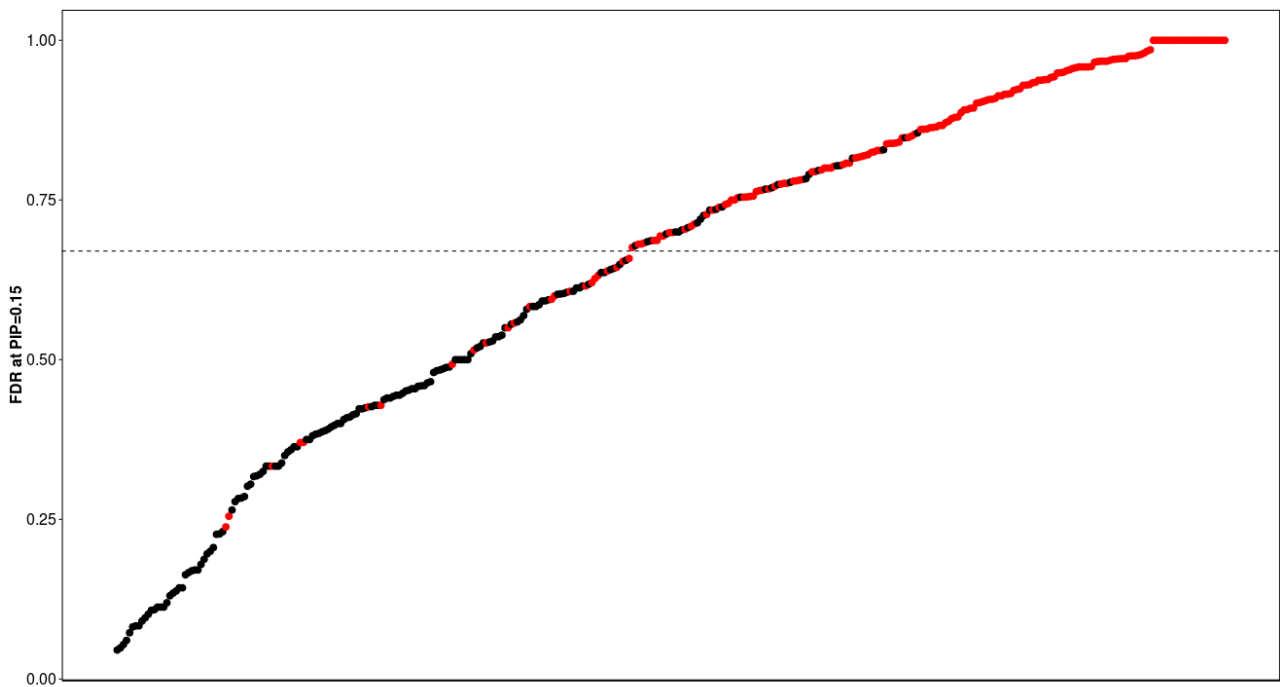
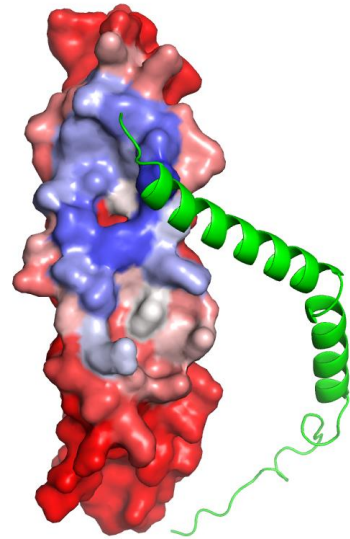
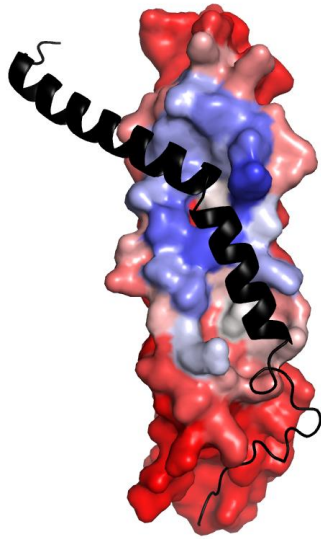
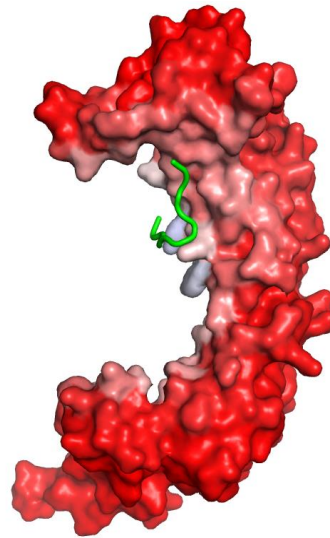
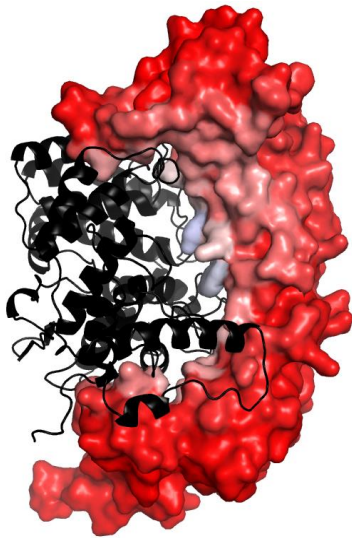


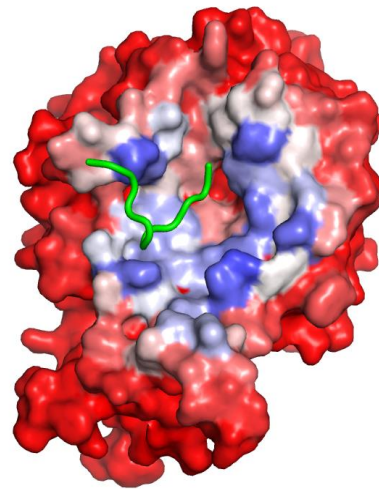
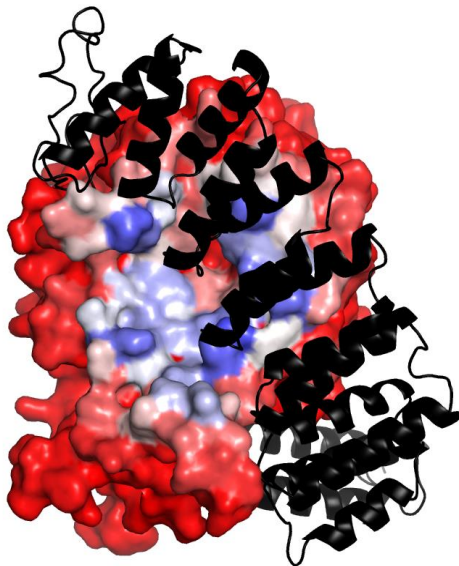
Figure S7 : Correlation between the visual protein inspection and the proteins FDR (FP/P) values computed at the optimal PIP cut-off of 0.15. The red dots represent proteins for which predicted alternate interfaces were visually observed by mapping the PIP values on the proteins' surface whereas the black dots point out proteins with no observed predicted alternate interface. Proteins were ordered according to their FDR values. The dot line represents the optimal FDR threshold of 0.67.



A

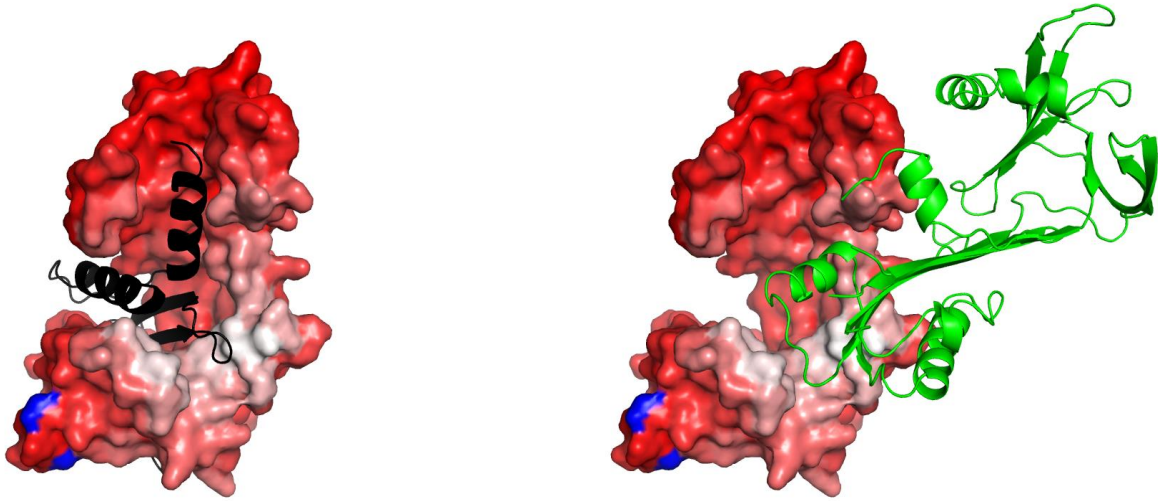


B

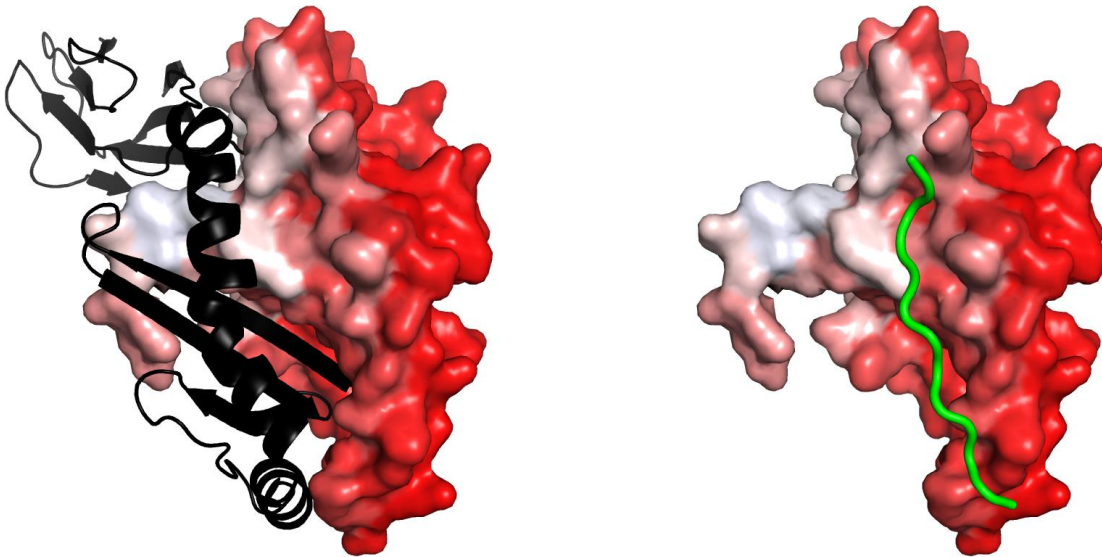


C

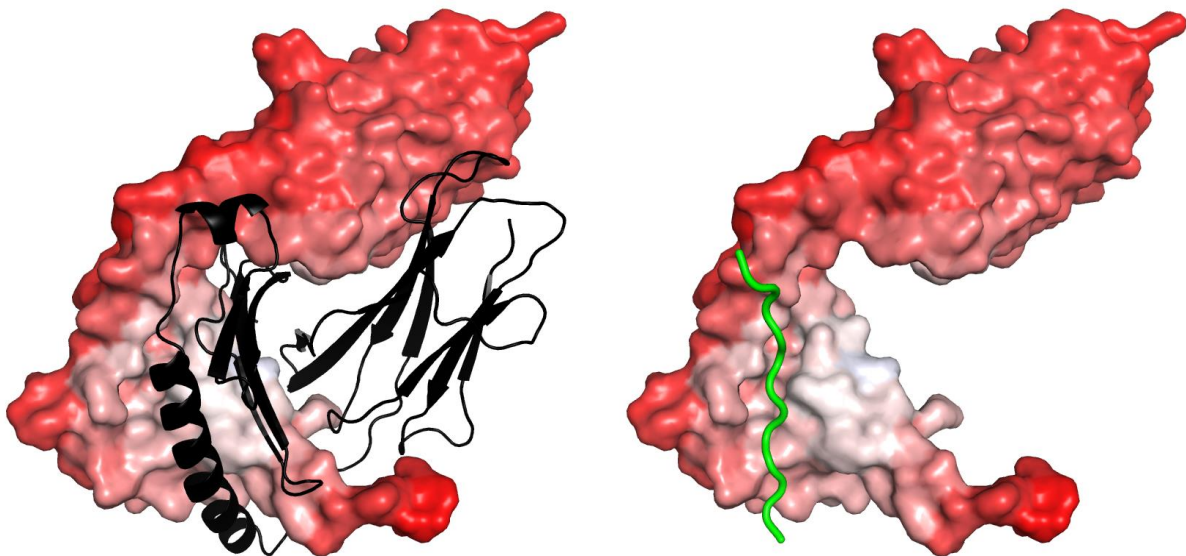
Figure S8 (continued next page)



D

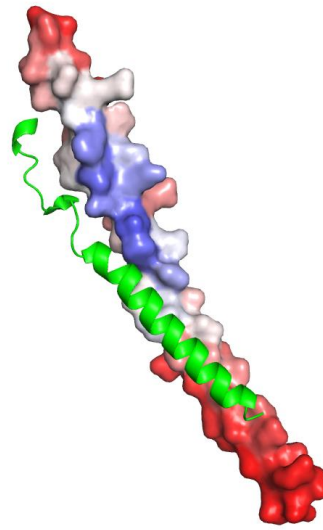
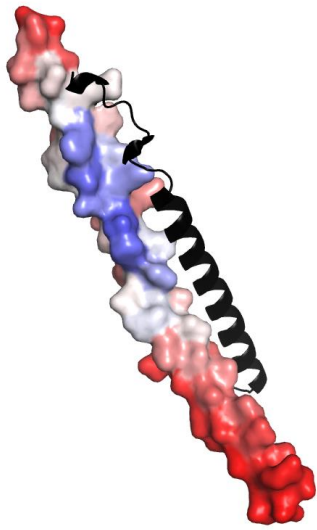


E

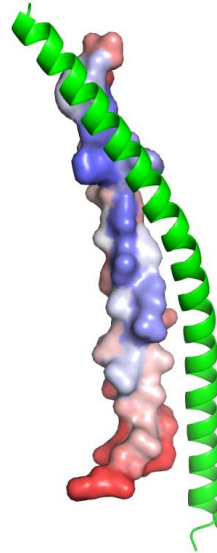
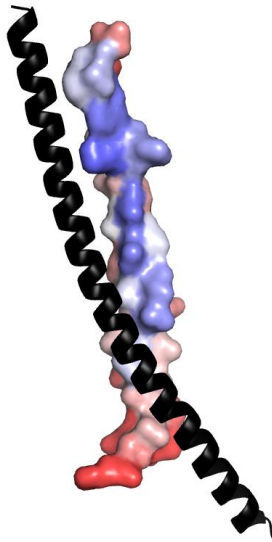


F

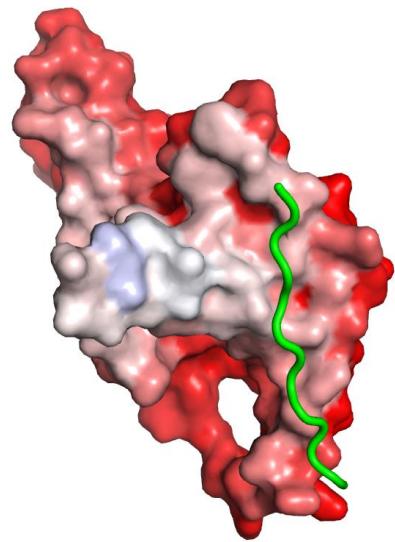
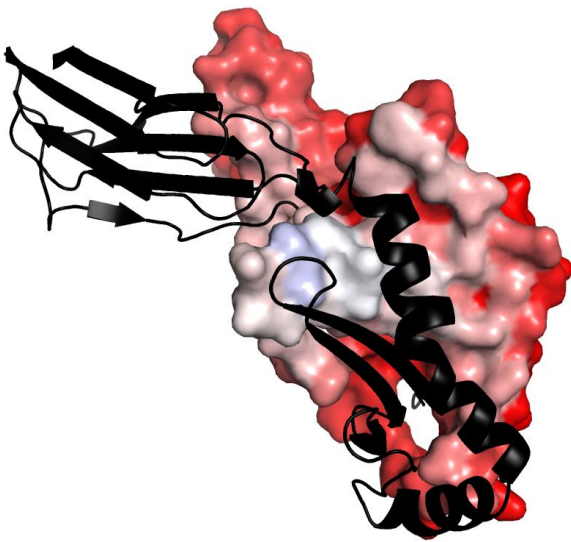
Figure S8 (continued next page)



G

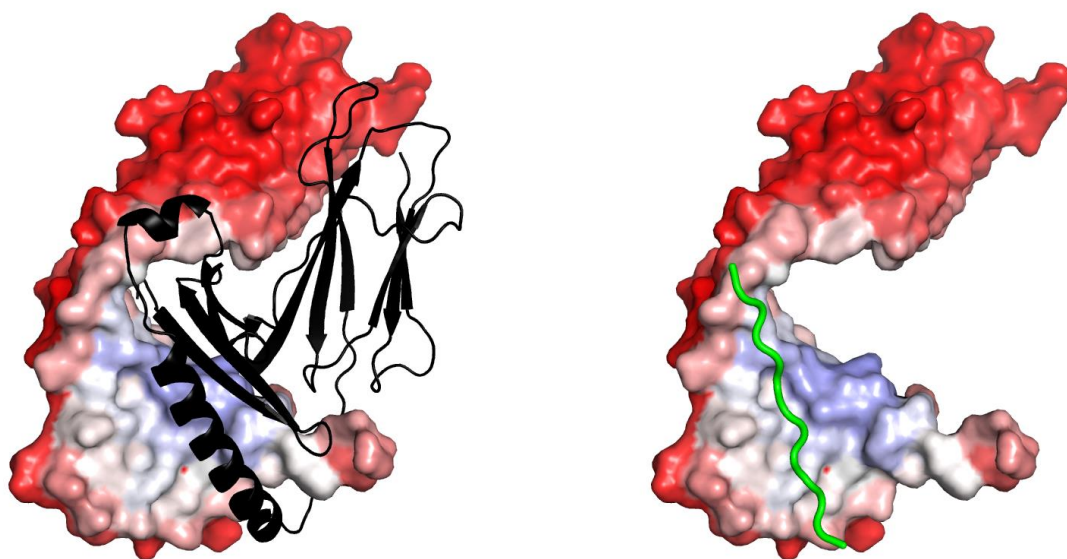


H



I

Figure S8 (continued next page)



J

Figure S8(A_J) : Mapping the PIP values on a protein's surface, high PIP residues are shown in blue and low PIP residues are shown in red. The reference experimental partner (ref) is shown in a black cartoon representation, while the alternate partner (proteic or peptidic) (alt) is shown in green.

(A) 1AVO_B with 1AVO_A(ref) and 1AVO_C(alt).

(B) 1D8D_A with 1D8D_B(ref) and 1D8D_P(alt).

(C) 1D8D_B with 1D8D_A(ref) and 1D8D_P(alt).

(D) 1JJO_C with 1JJO_A(ref), 1JJO_E(ref) and 1JJO_D(alt).

(E) 2NNA_A with 2NNA_B(ref) and 2NNA_C(alt).

(F) 2NNA_B with 2NNA_A(ref) and 2NNA_C(alt).

(G) 3BRT_B with 3BRT_C(ref) and 3BRT_A(alt).

(H) 3BRT_C with 3BRT_B(ref) and 3BRT_D(alt).

(I) 3C5J_A with 3C5J_B(ref) and 3C5J_C(alt).

(J) 3C5J_B with 3C5J_A(ref) and 3C5J_C(alt)

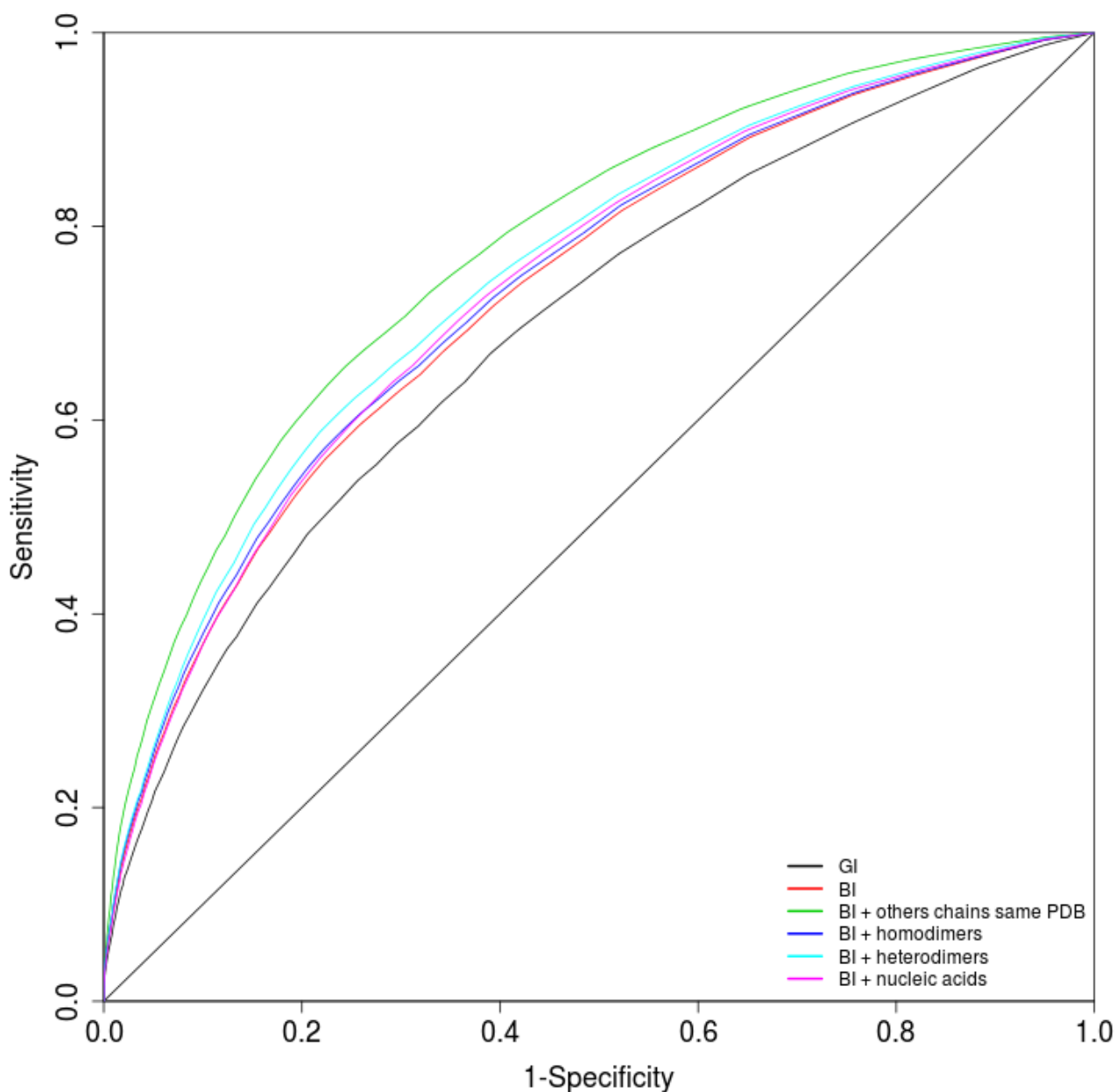
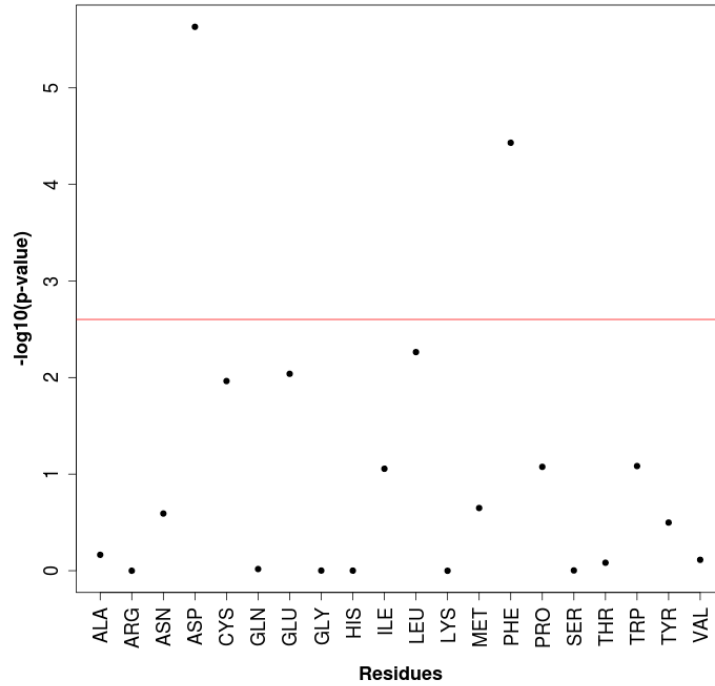
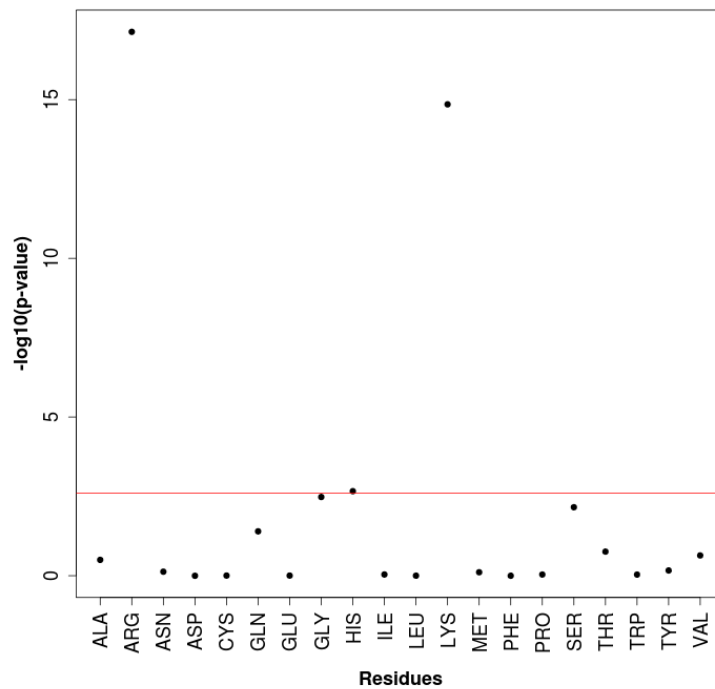


Figure S9 : ROC curves of the PIP prediction obtained with the GI score with the reference experimental interfaces (REI) (black line), with the BI score with the REI (red line), with the BI score with REI and alternate experimental interfaces from other chains of the same PDB (green line), with the BI score with REI and alternate experimental interfaces from homodimers (blue line), with the BI score with REI and alternate experimental interfaces from heteromdimers (cyan line) and with the BI score with REI and alternate nucleic acid experimental interfaces (magenta line). The diagonal dotted line corresponds to random prediction.

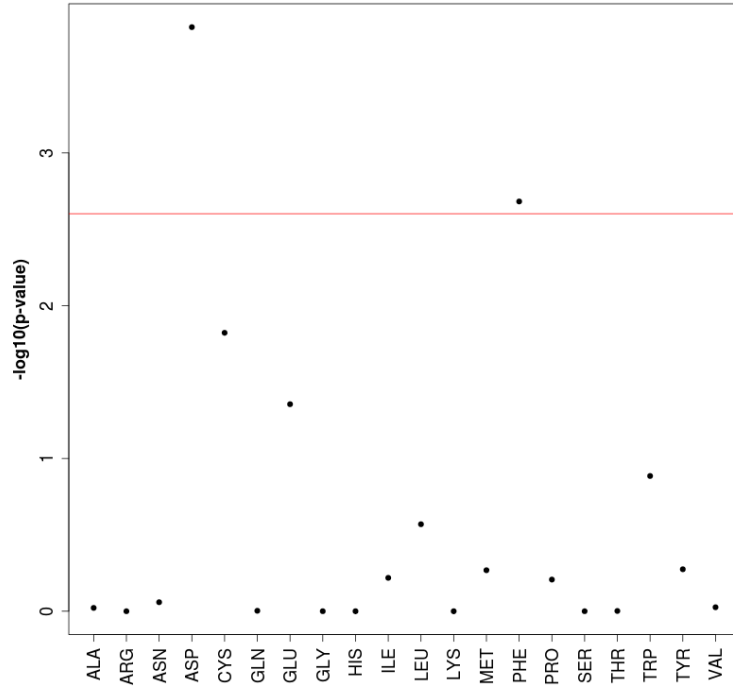


A

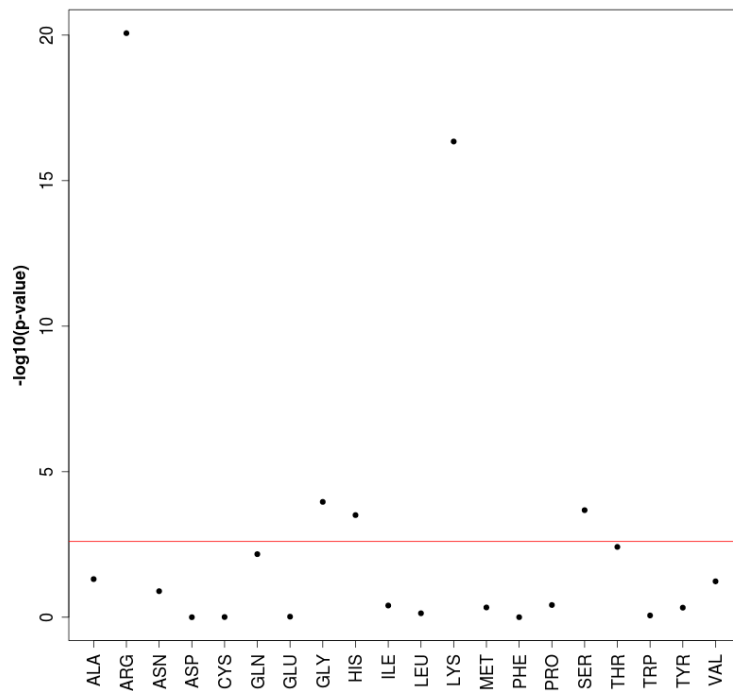


B

Figure S10 : Residues are plotted as the distribution of the negative logarithmic p-value ($-\log_{10}(\text{p-value})$) of the one-tailed Wilcoxon test for the fraction of each residue type in the interface (FRires(type)) (A) option « less », (B) option « greater ». All dots located above the Bonferroni threshold (red line) display a mean value significantly inferior (A) or superior (B) in the NAI than in the PPI.

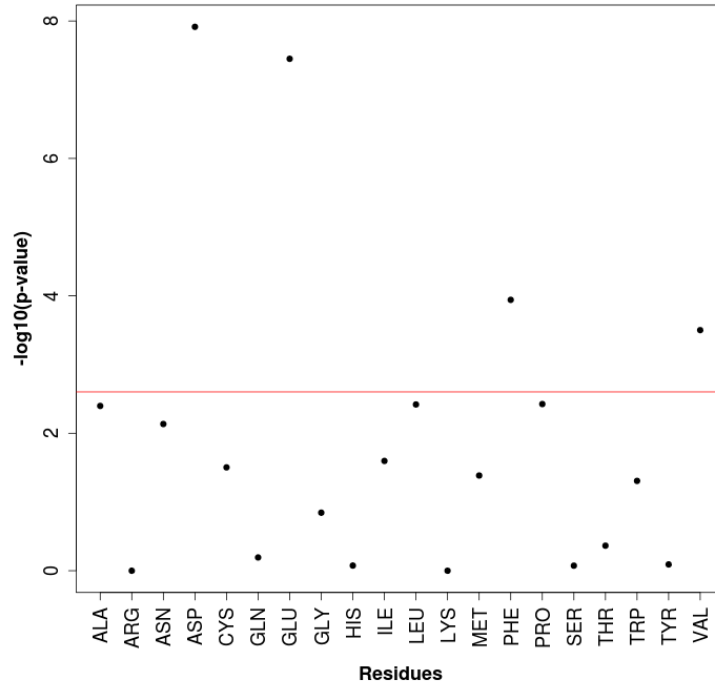


A

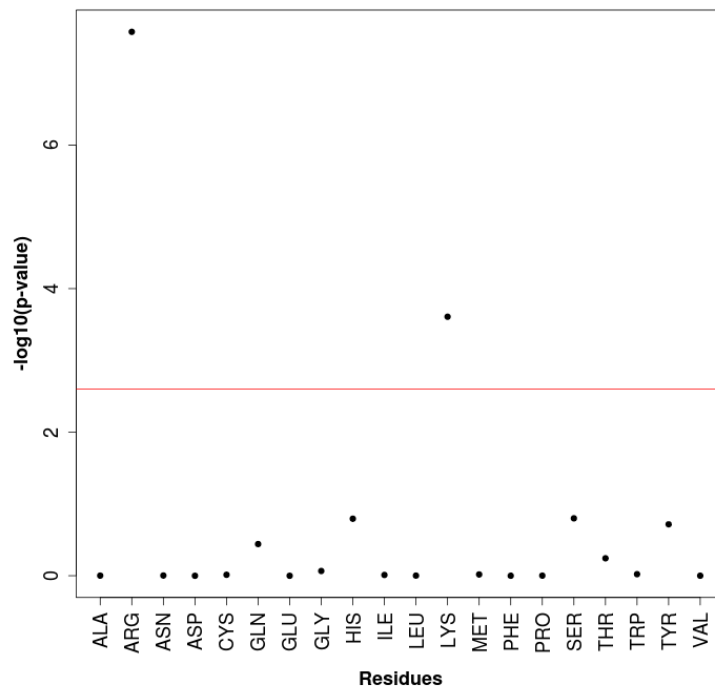


B

Figure S11 : Residues are plotted as the distribution of the negative logarithmic p-value ($-\log_{10}(\text{p-value})$) of the one-tailed Wilcoxon test for the number of each residue type in the interface (A) option « less », (B) option « greater ». All dots located above the Bonferroni threshold (red line) display a mean value significantly inferior (A) or superior (B) in the NAI than in the PPI.

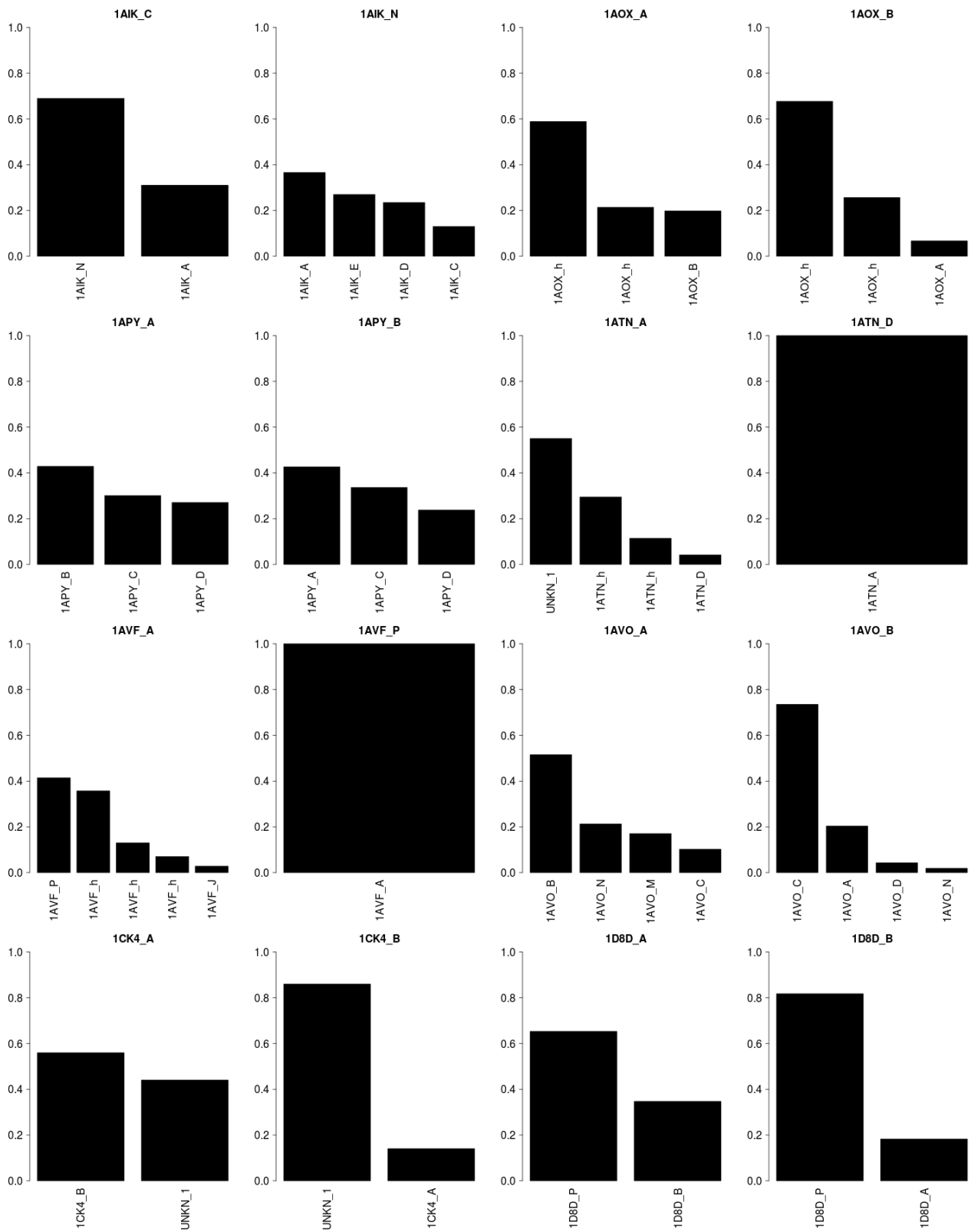


A

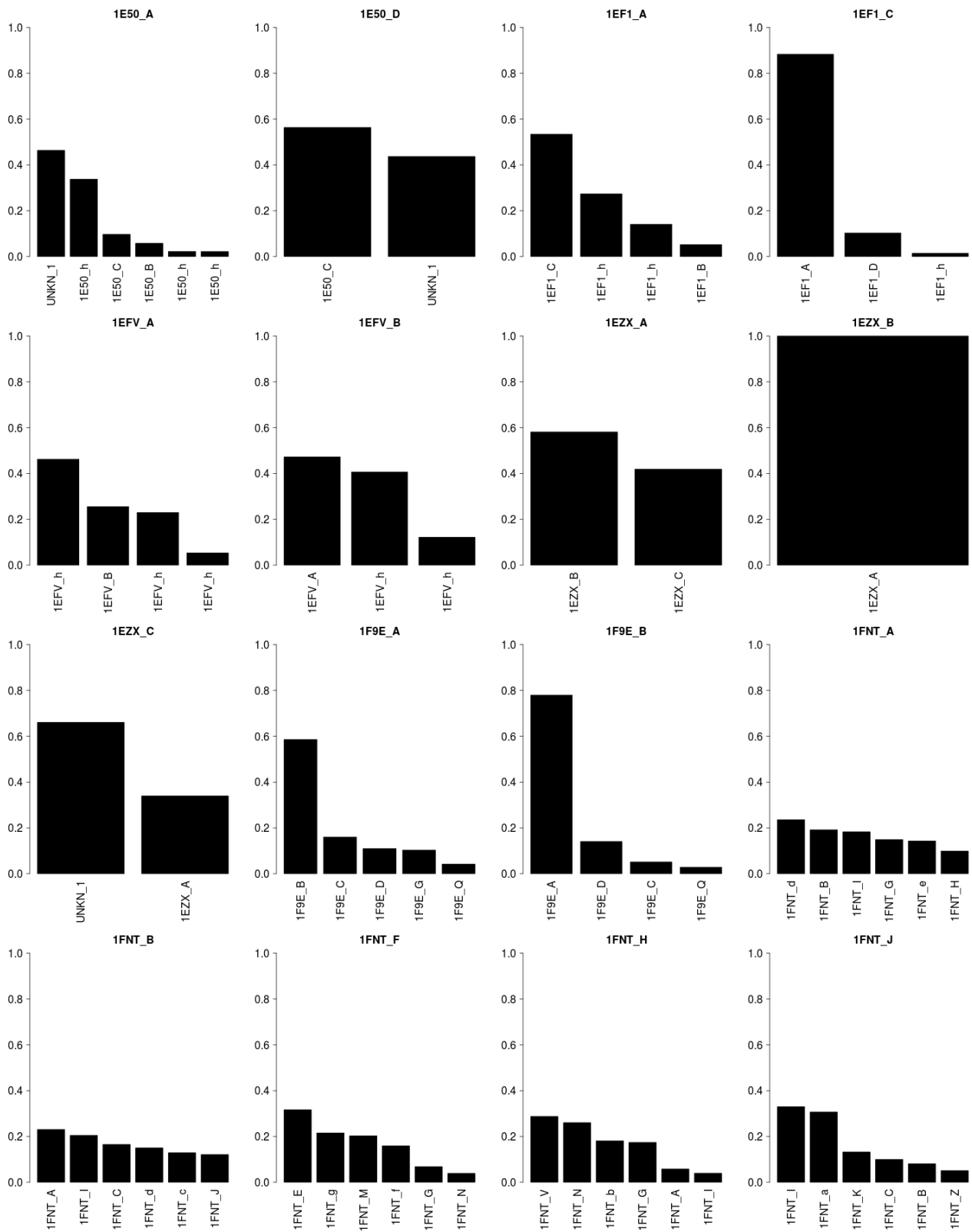


B

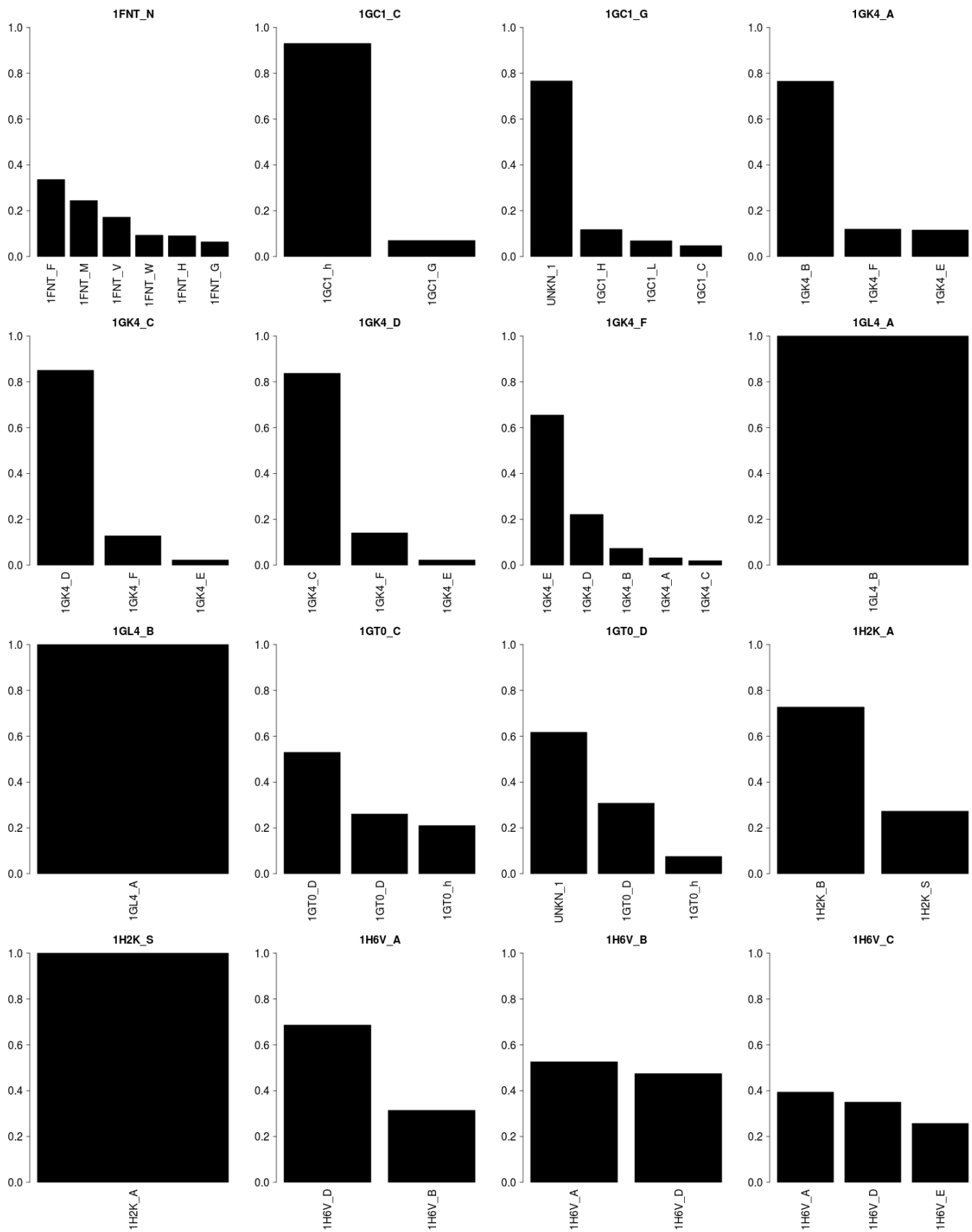
Figure S12 : Residues are plotted as the distribution of the negative logarithmic p-value ($-\log_{10}(\text{p-value})$) of the one-tailed Wilcoxon test for the fraction of each residue type in the interface ($\text{FRI}_{\text{res}(\text{type})}$) in the NAI compared to the fraction of each residue type observed in the whole corresponding protein surface ($\text{FRI}_{\text{res}(\text{type})[\text{surface}]}$) (A) option « less », (B) option « greater ». All dots located above the Bonferroni threshold (red line) display a mean value significantly inferior (A) or superior (B) in the NAI than in the whole protein surface.



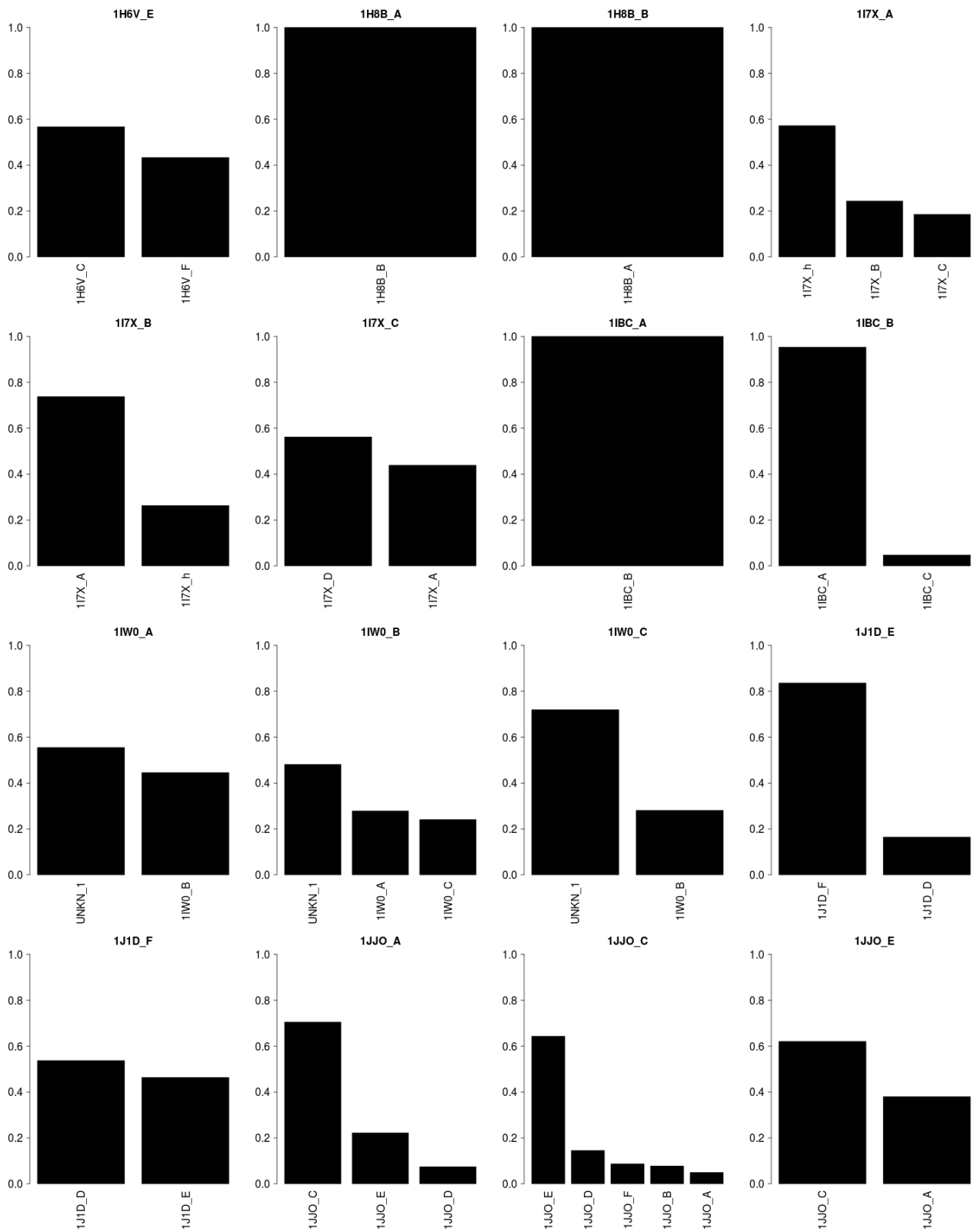
A
Figure S13 (continued next page)



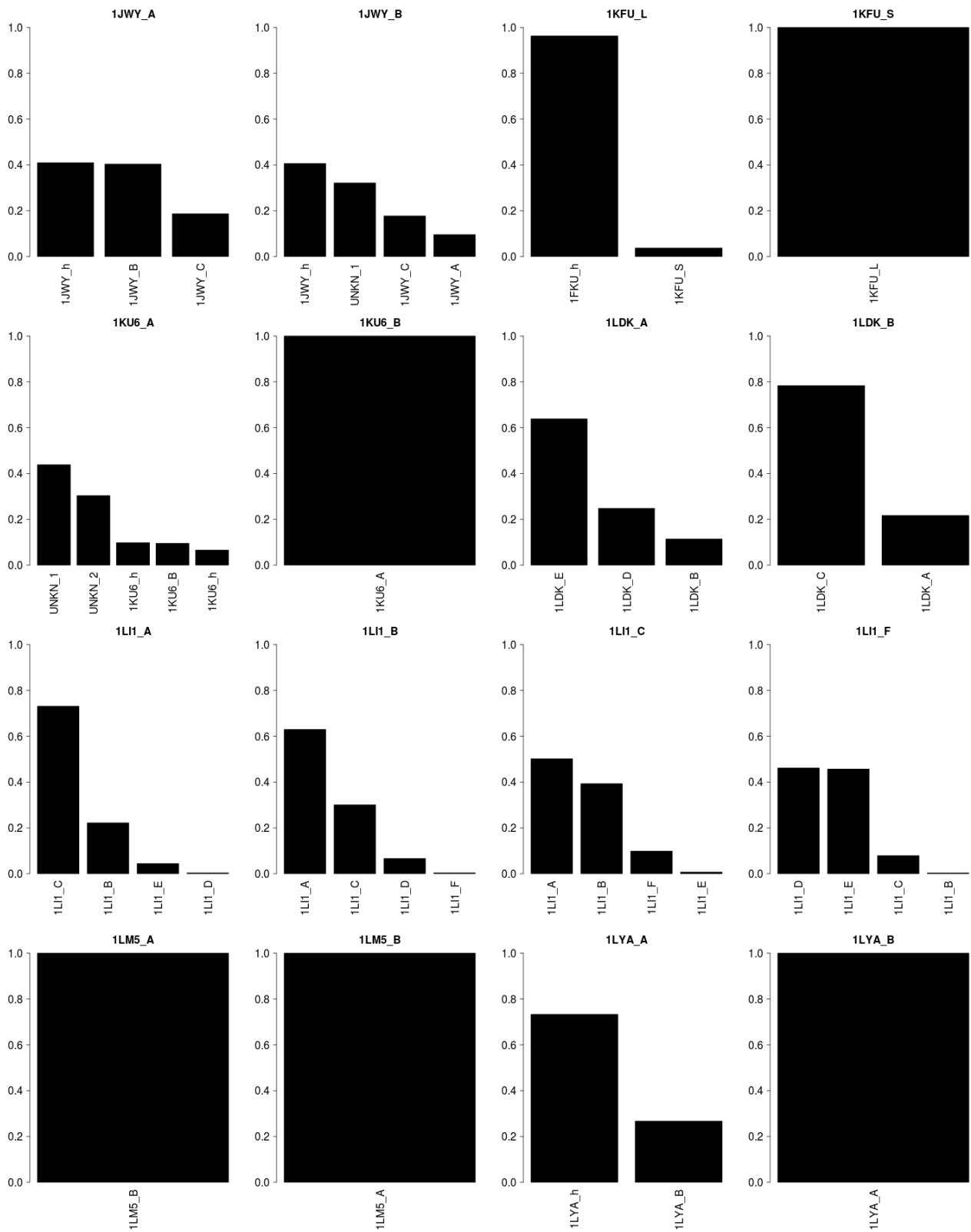
B
Figure S13 (continued next page)



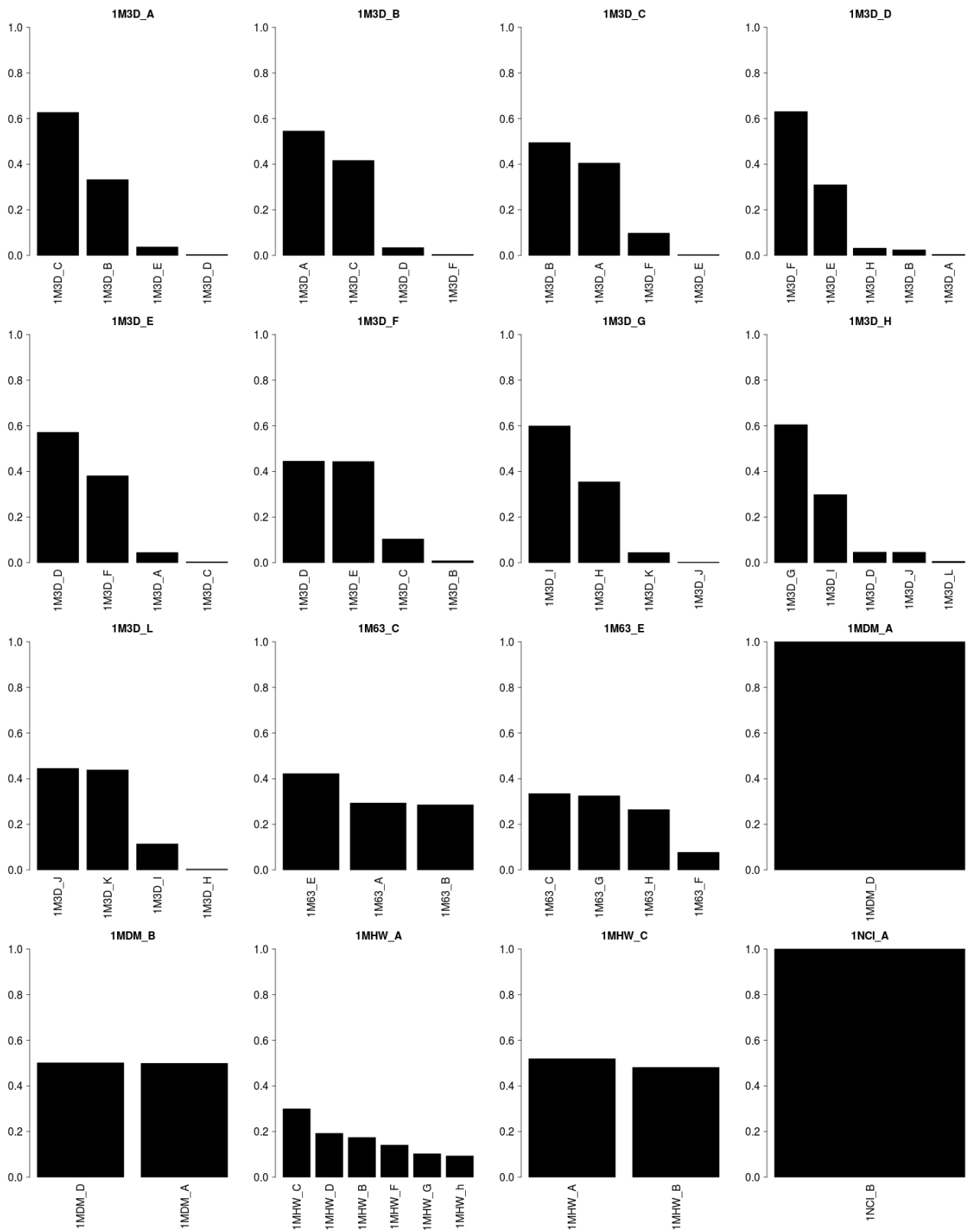
C
Figure S13 (continued next page)



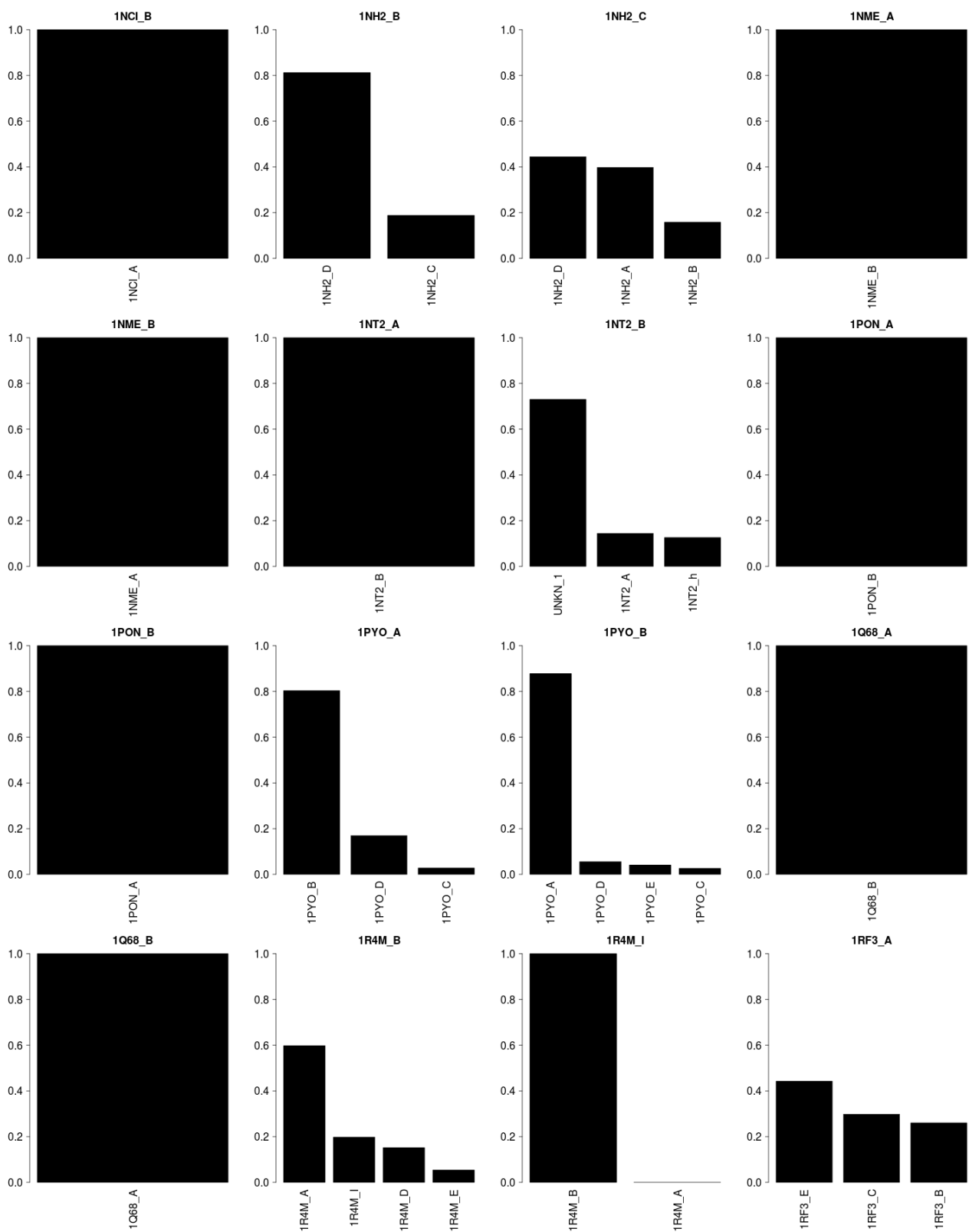
D
Figure S13 (continued next page)



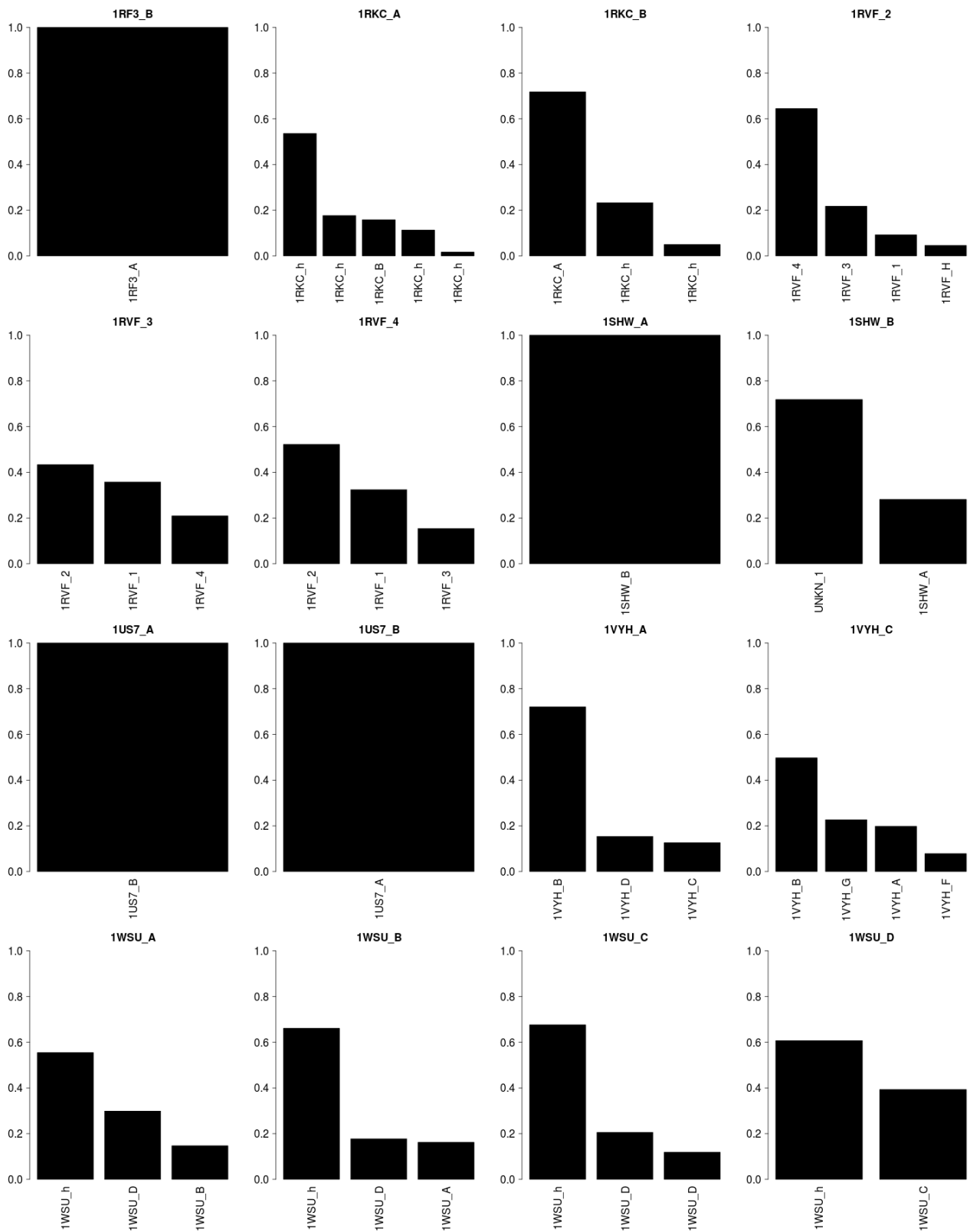
E
Figure S13 (continued next page)



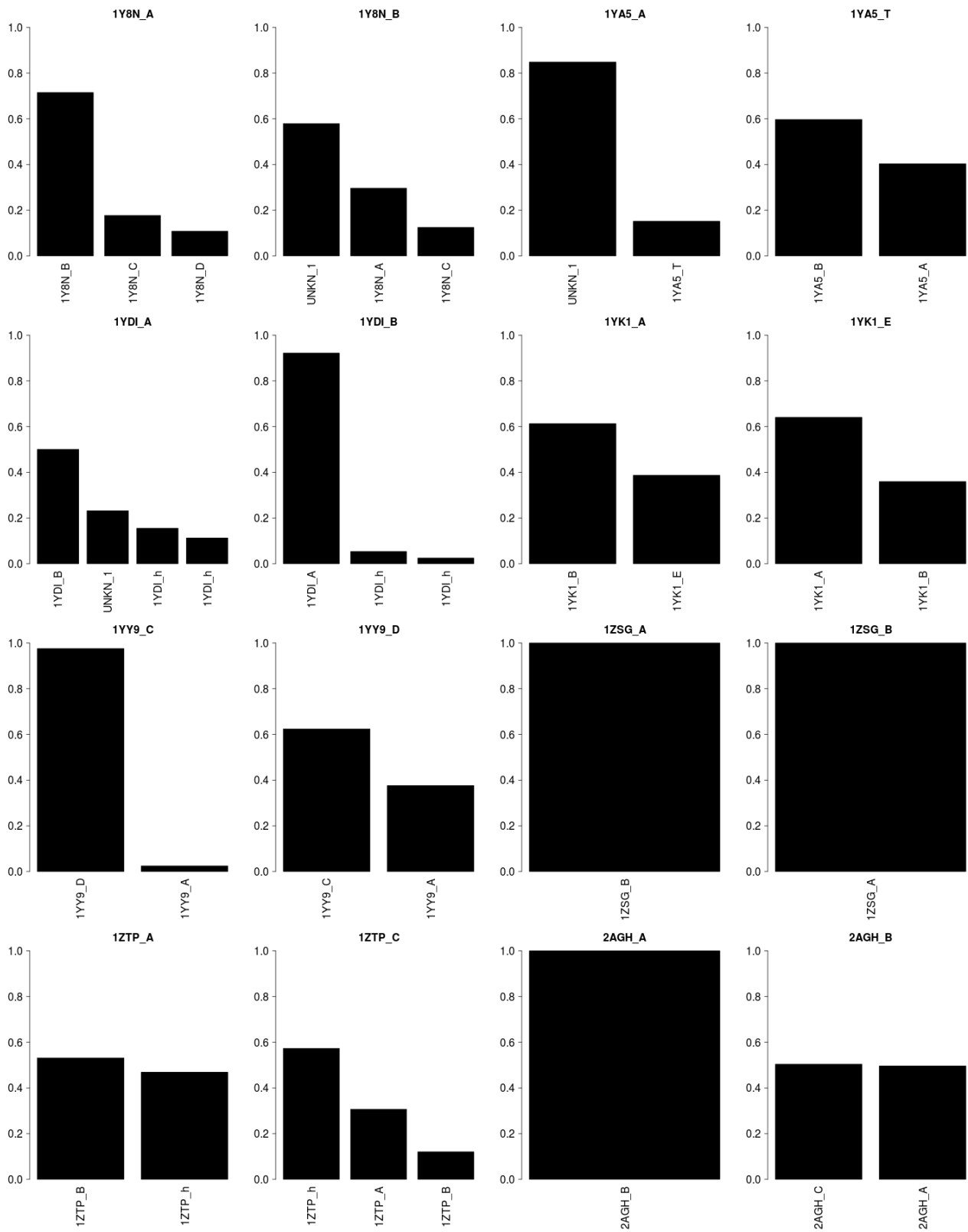
F
Figure S13 (continued next page)



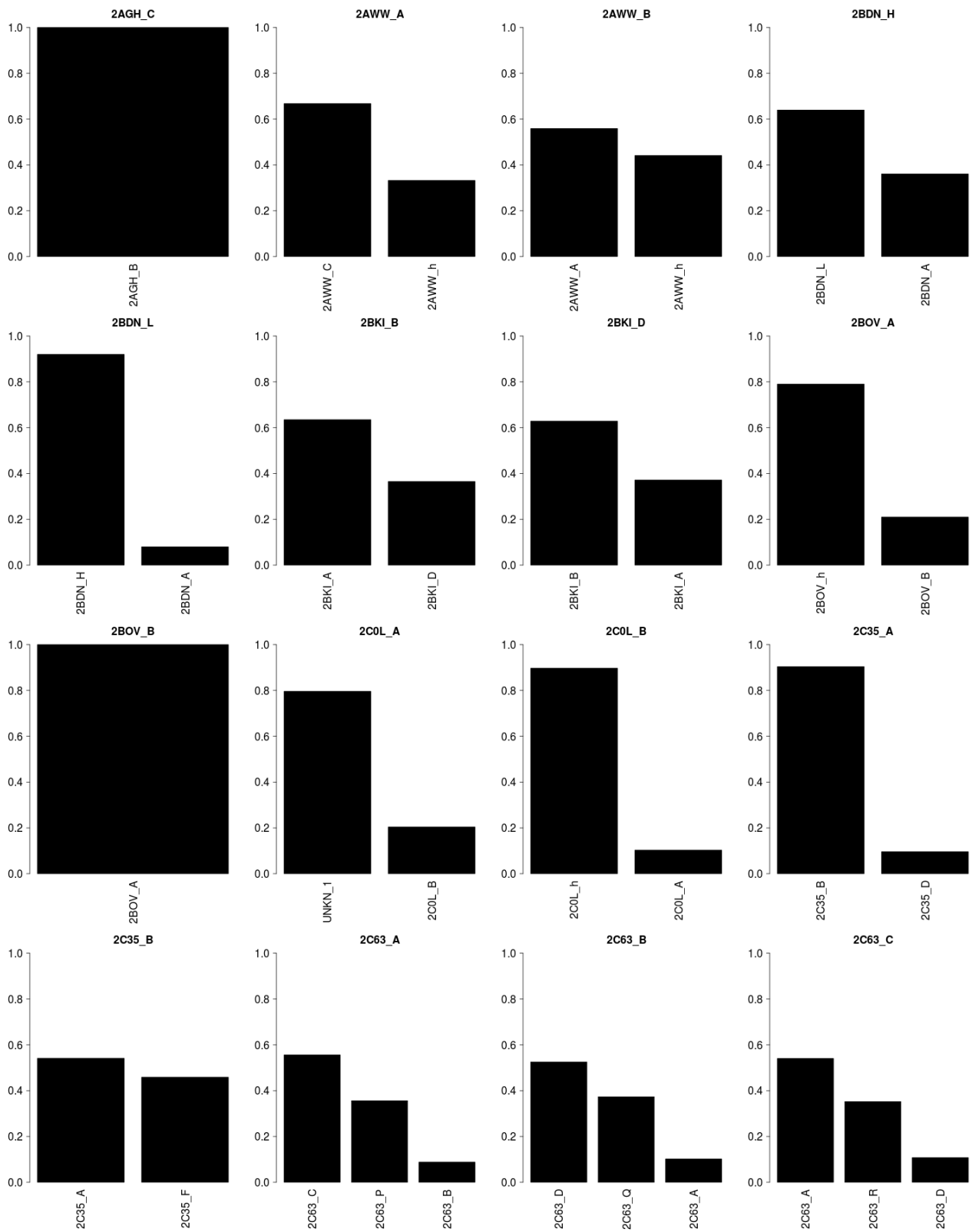
G
Figure S13 (continued next page)



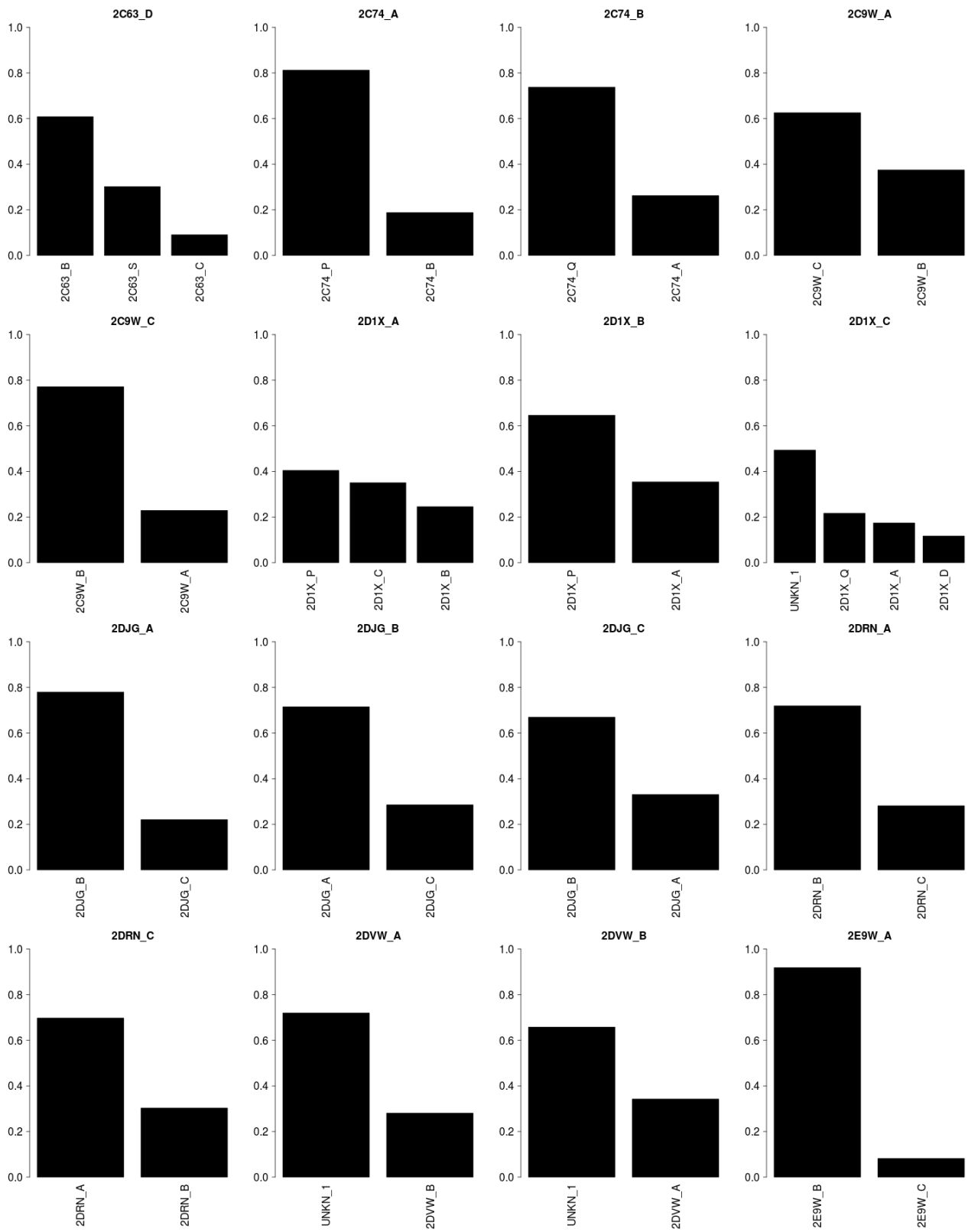
H
Figure S13 (continued next page)



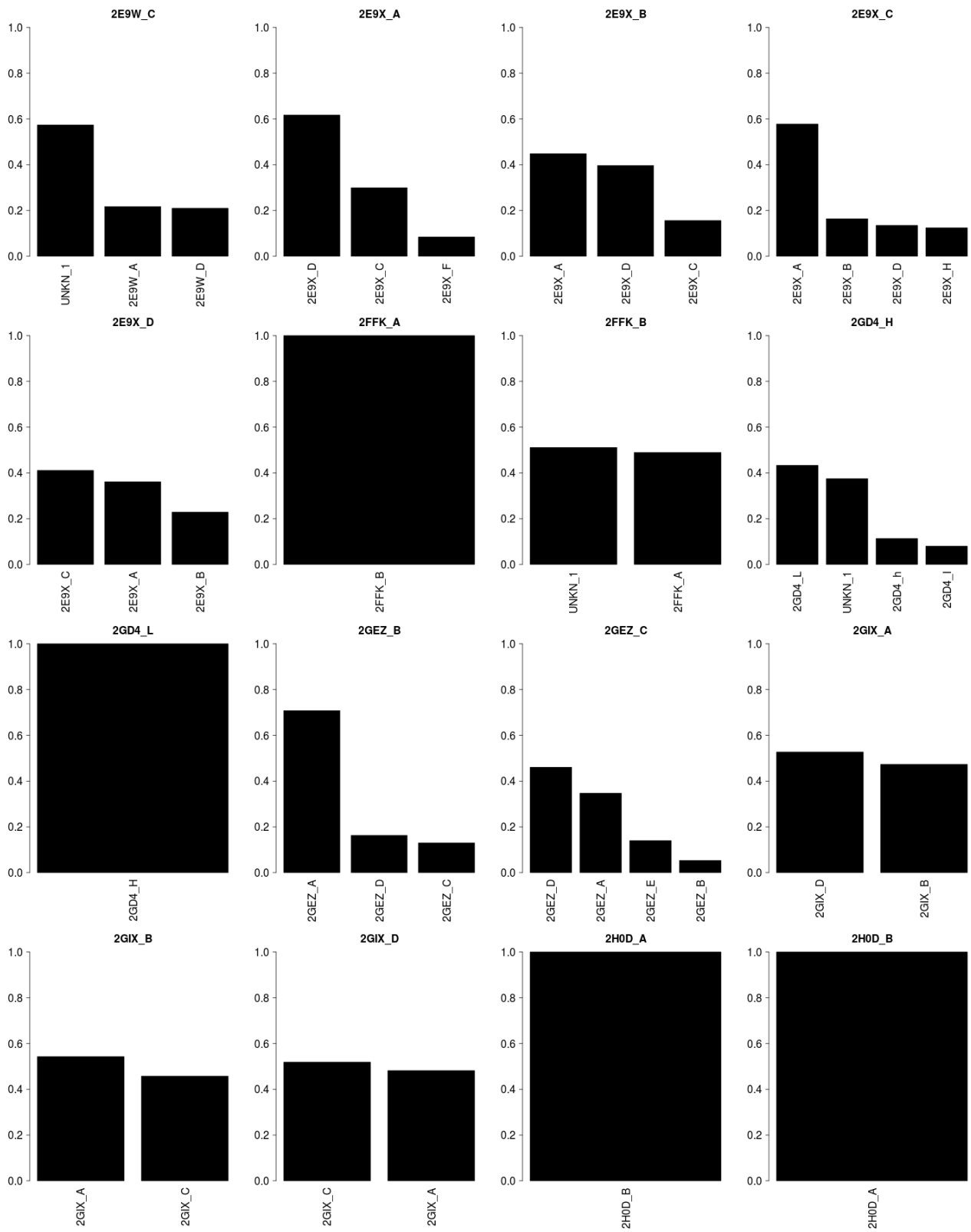
I
Figure S13 (continued next page)



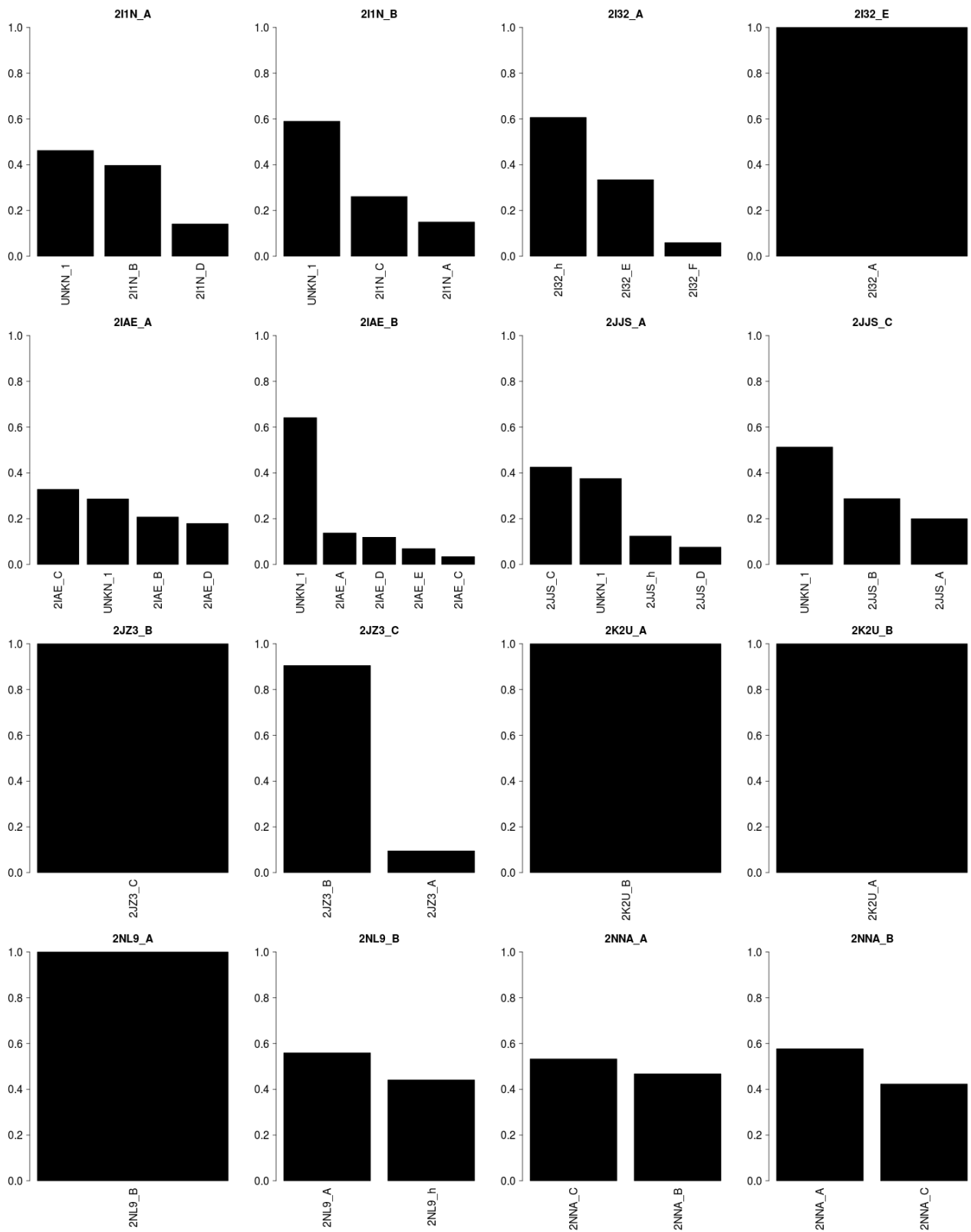
J
Figure S13 (continued next page)



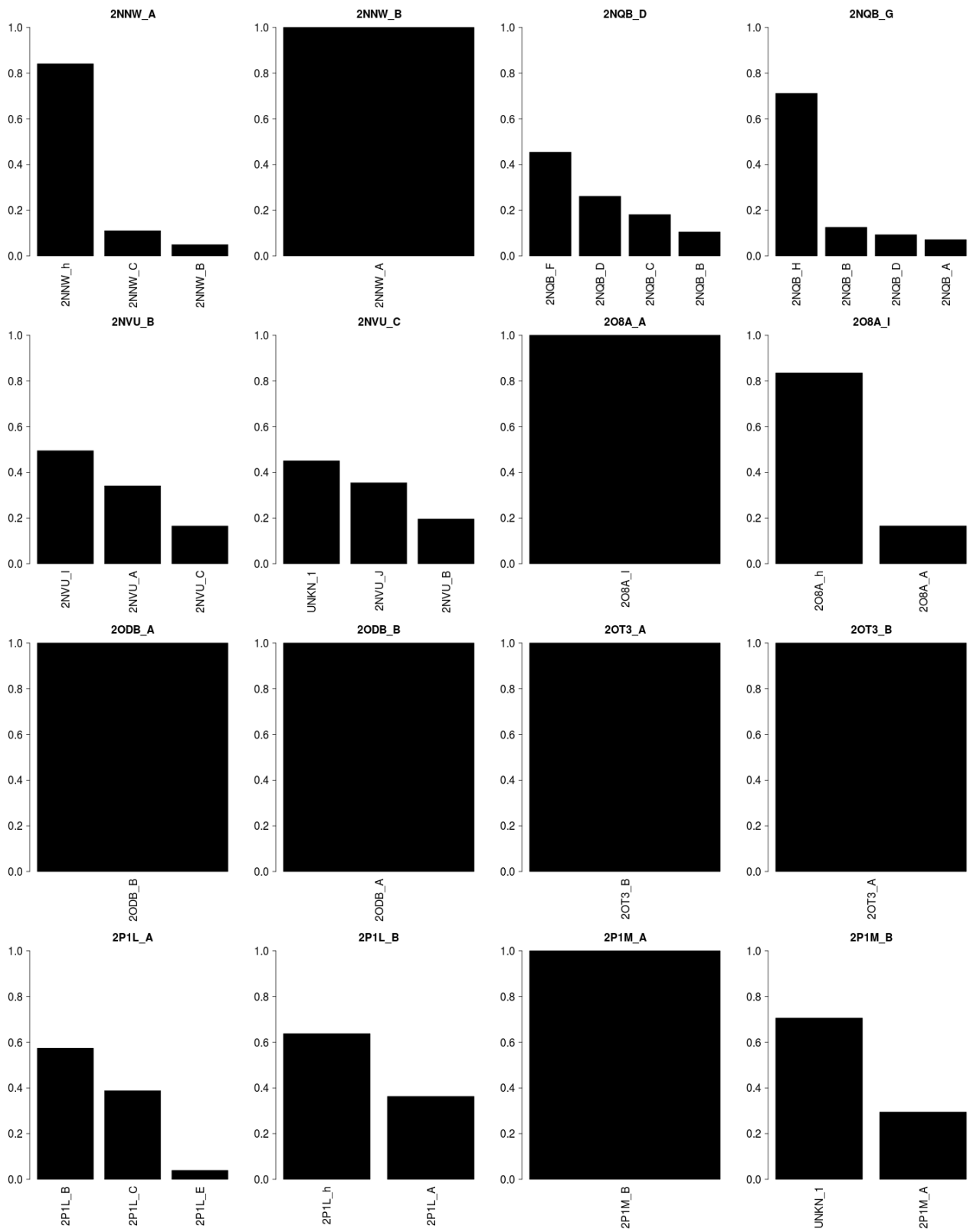
K
Figure S13 (continued next page)



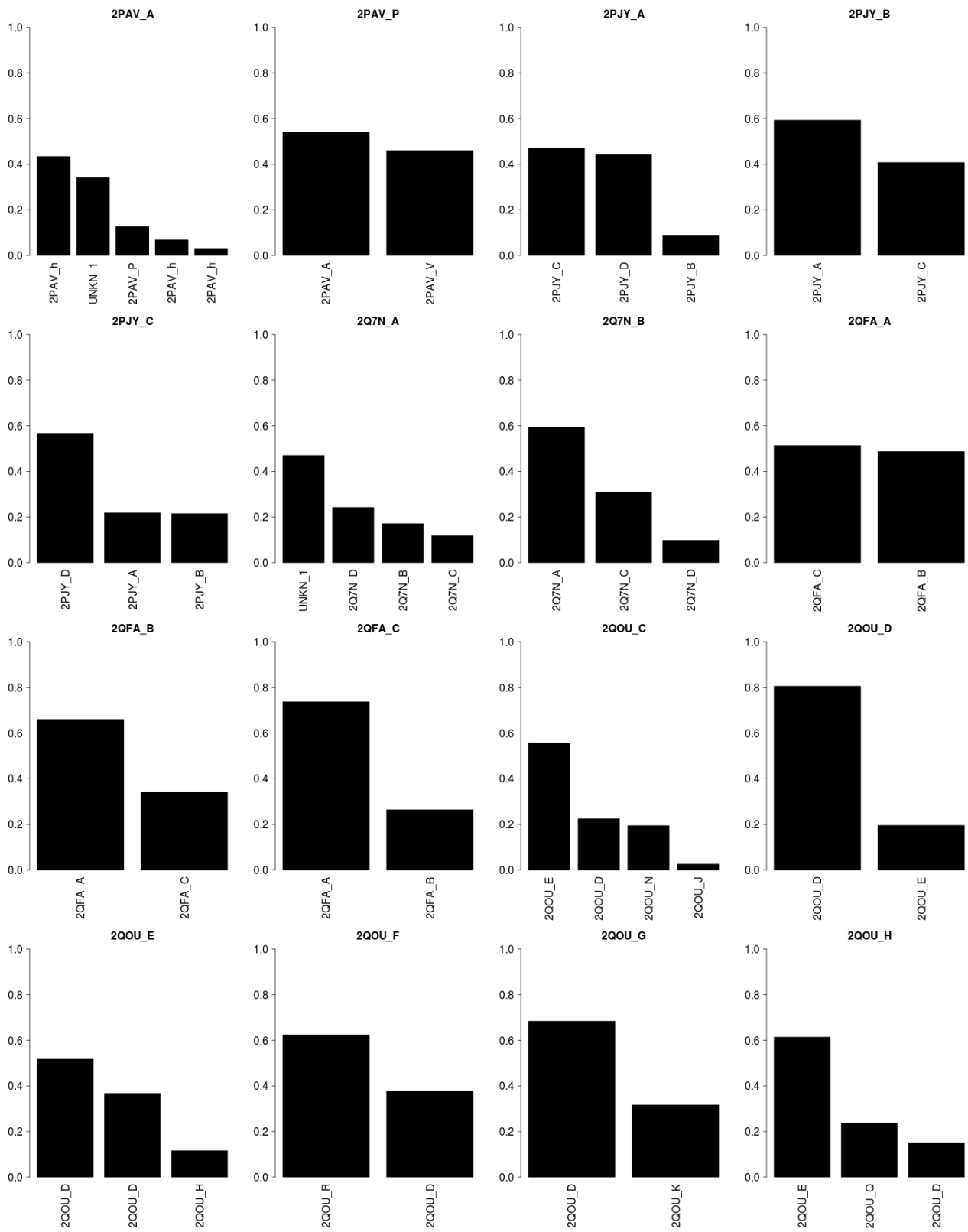
L
Figure S13 (continued next page)



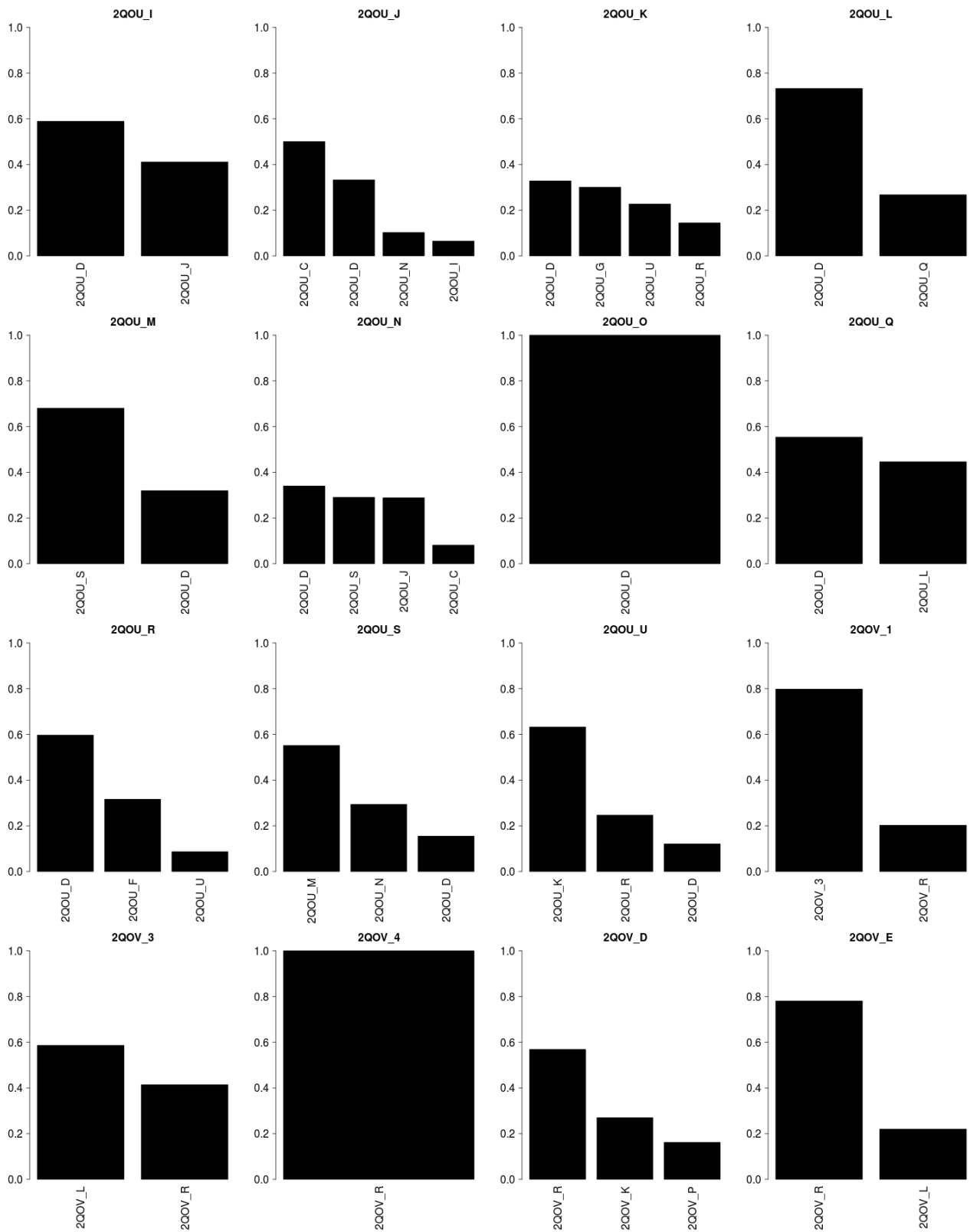
M
Figure S13 (continued next page)



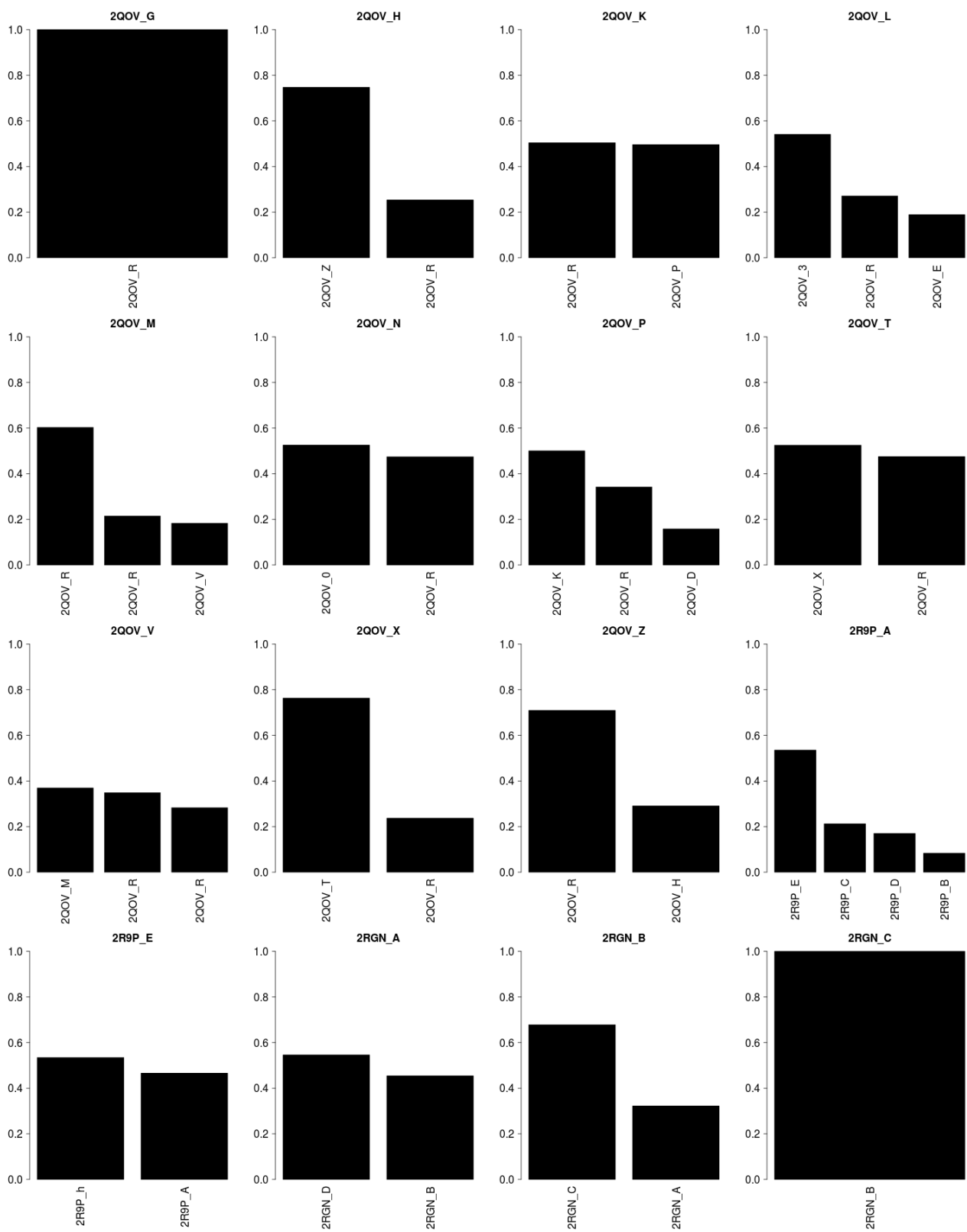
N
Figure S13 (continued next page)



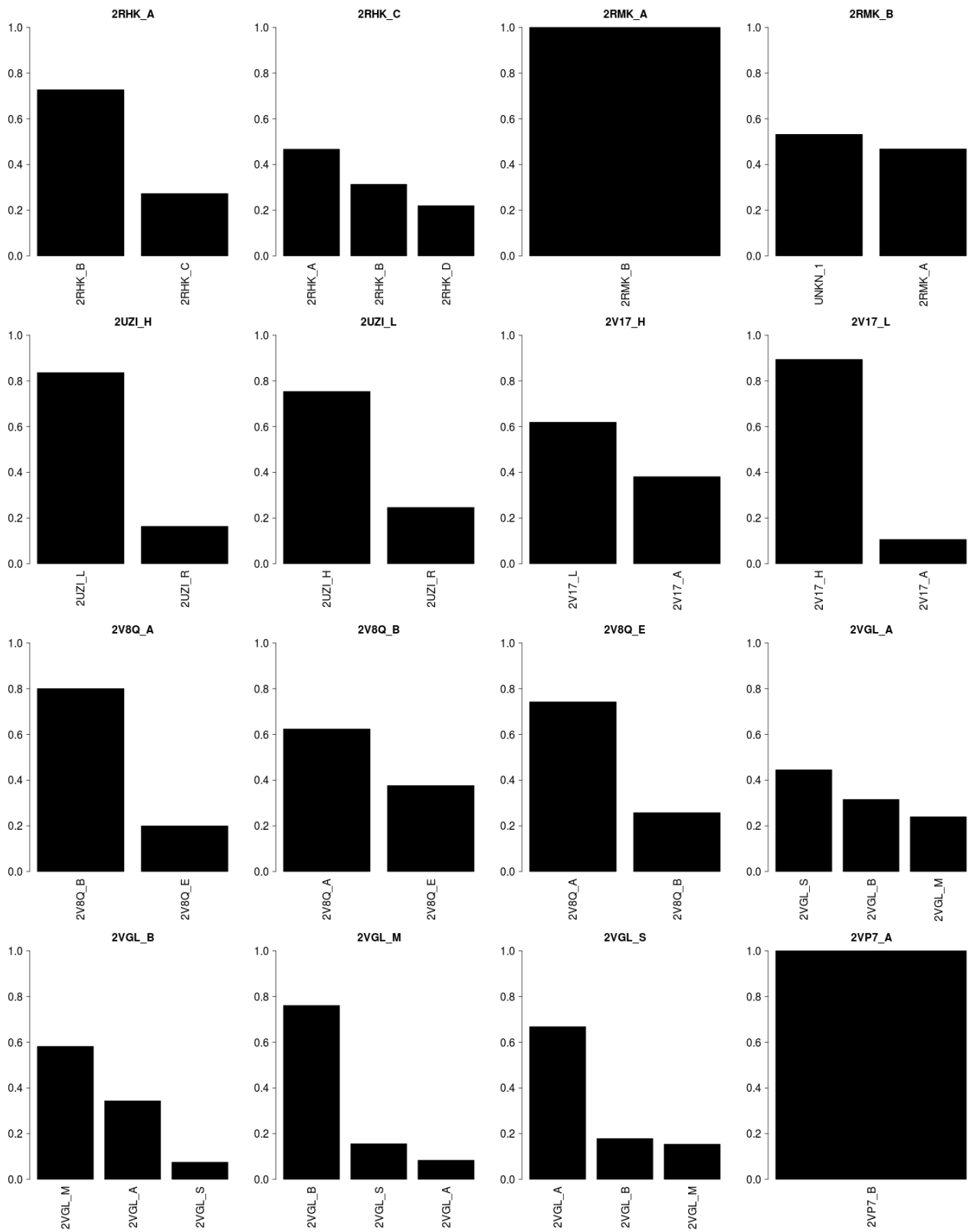
O
Figure S13 (continued next page)



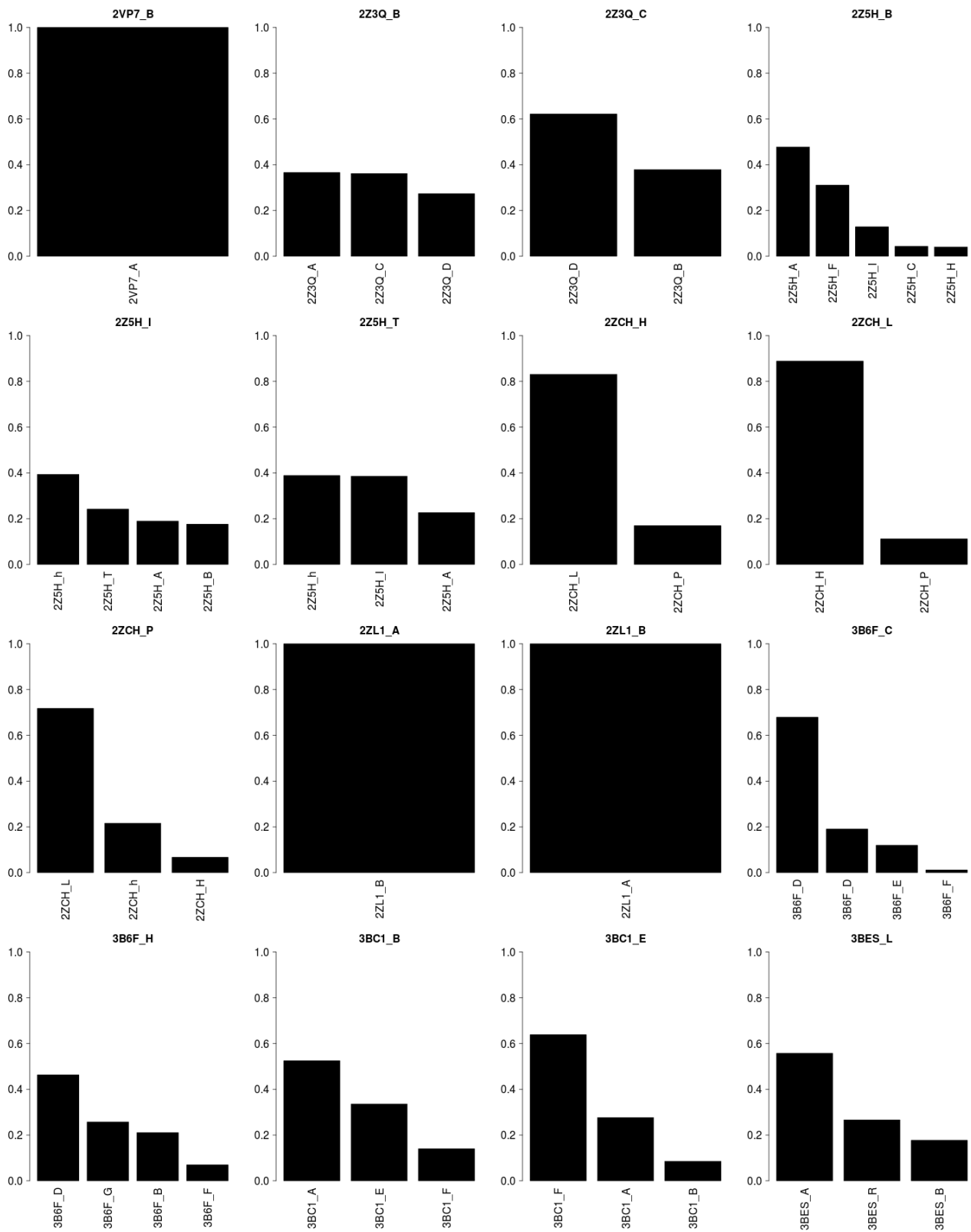
P
Figure S13 (continued next page)



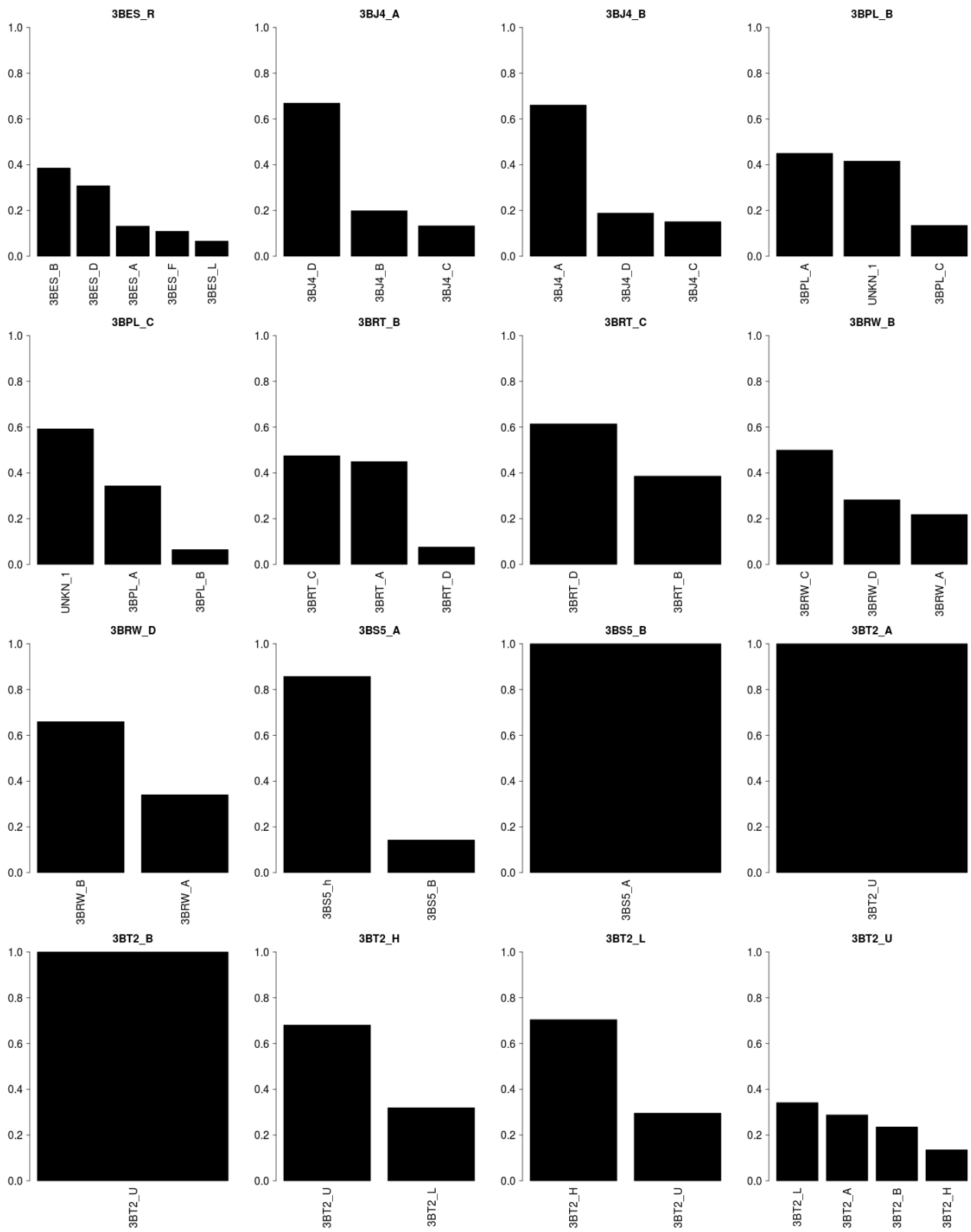
Q
Figure S13 (continued next page)



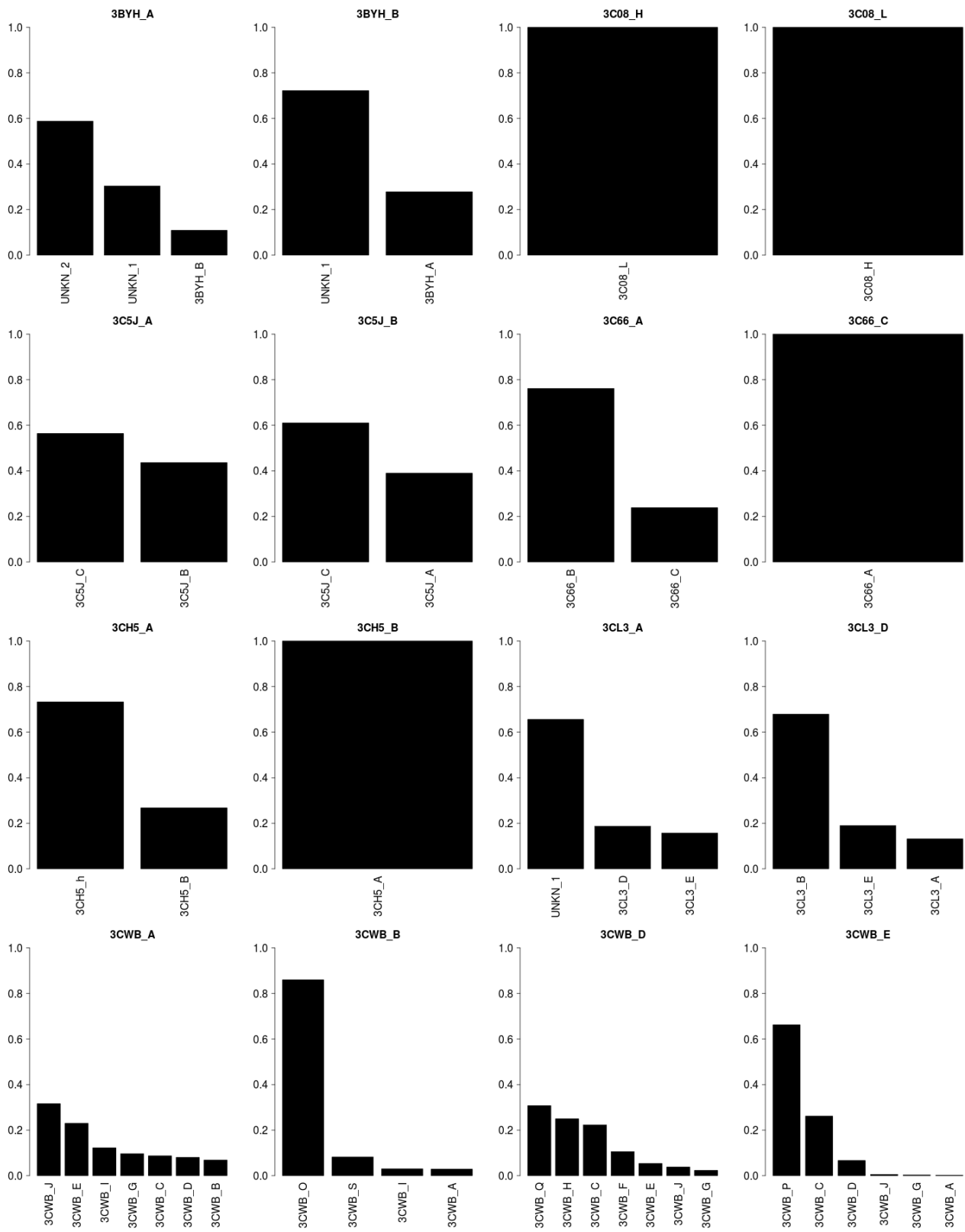
R
Figure S13 (continued next page)



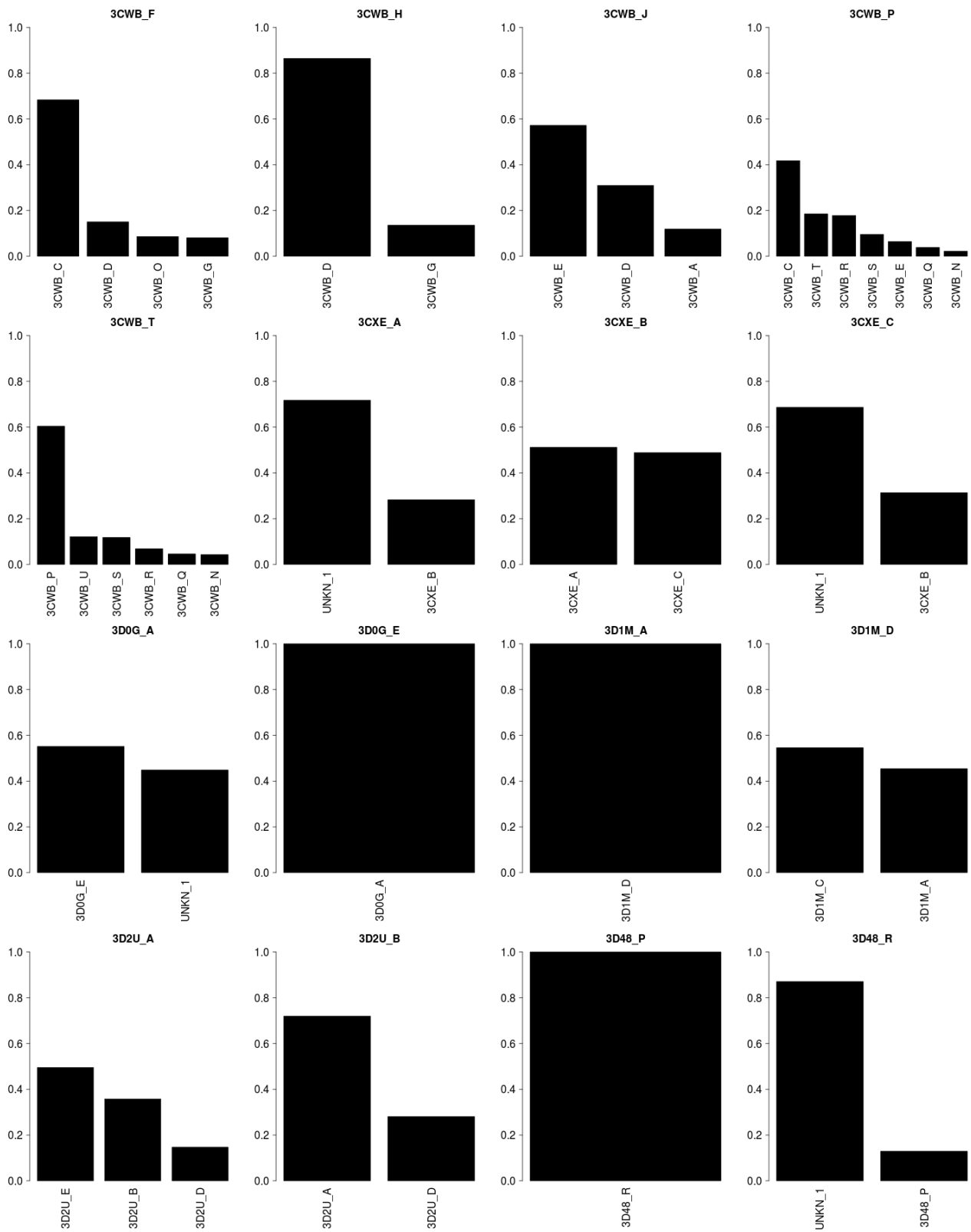
S
Figure S13 (continued next page)



T
Figure S13 (continued next page)

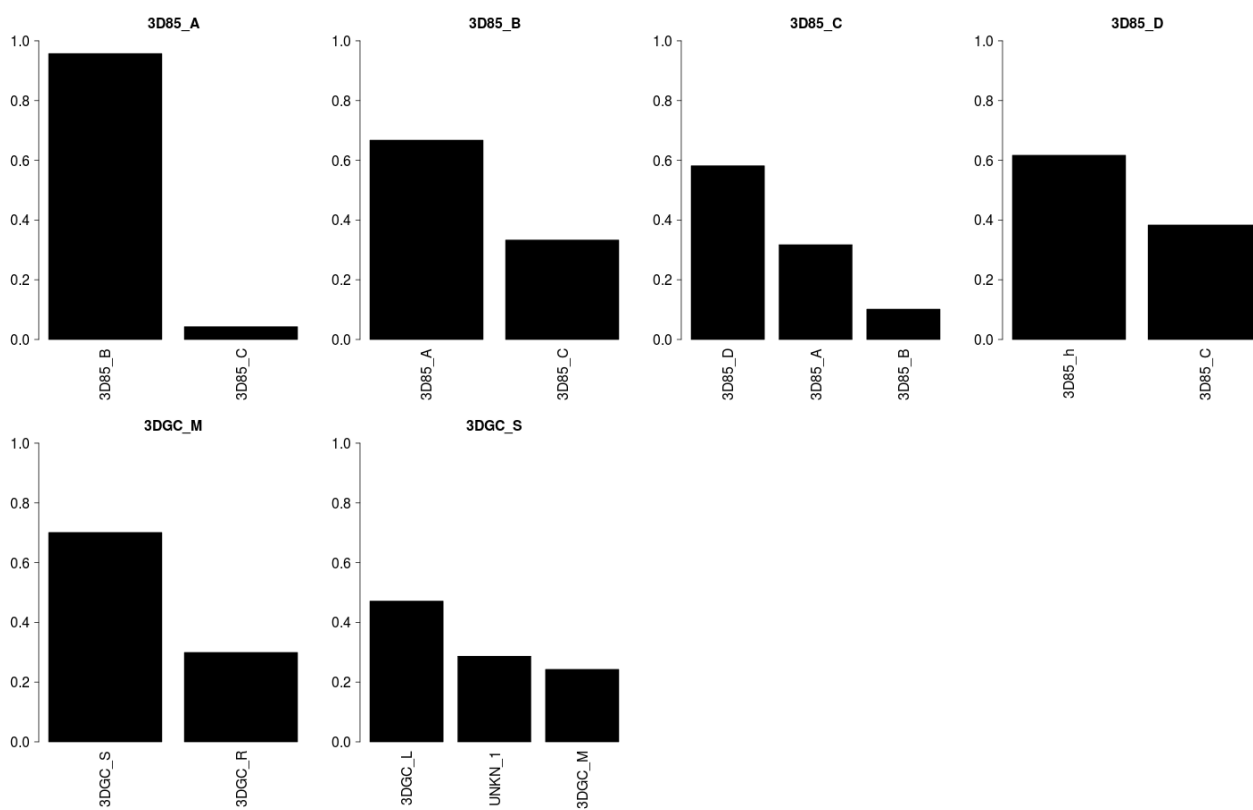


U
Figure S13 (continued next page)



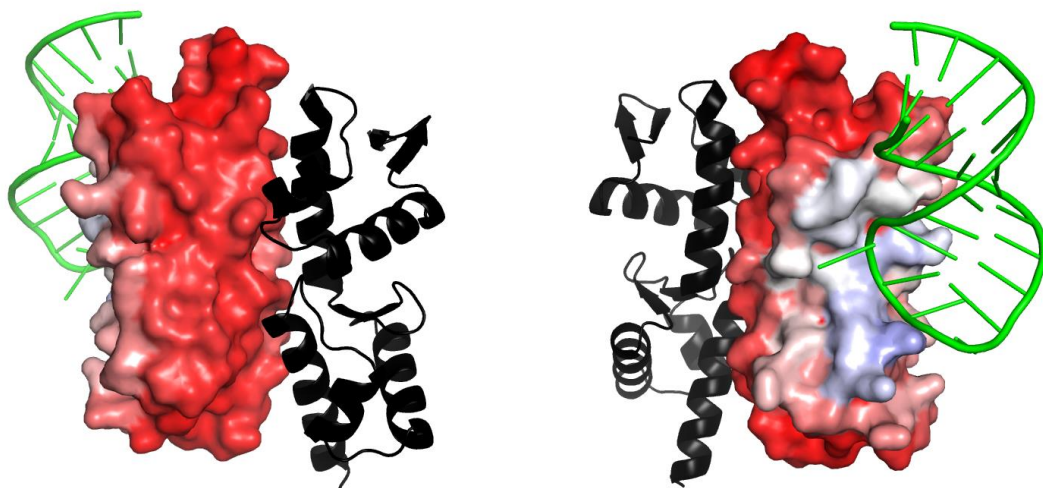
V

Figure S13 (continued next page)

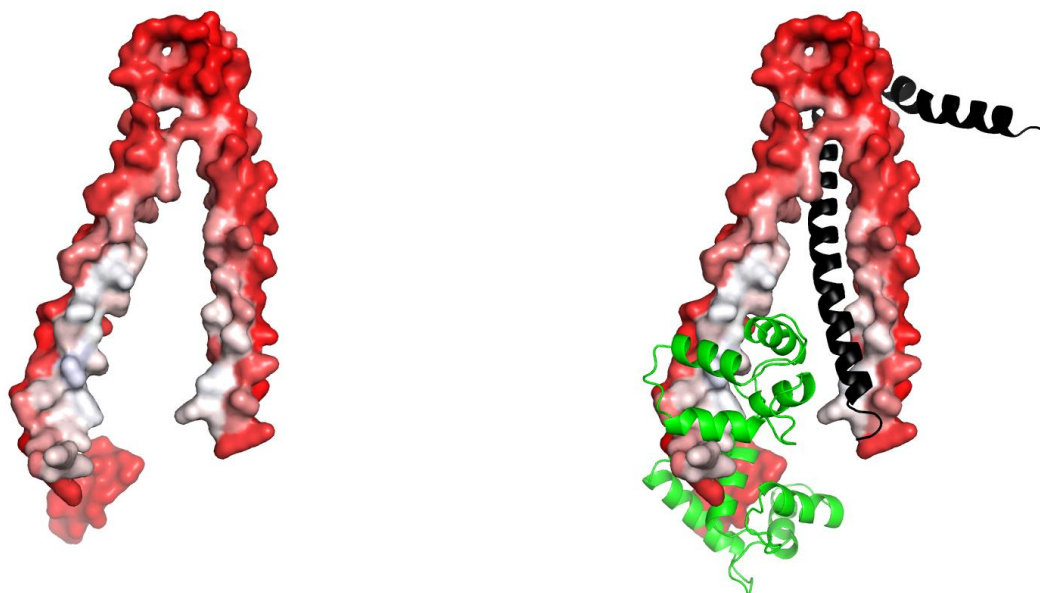


W

Figure S13(A-W) : Occupancy rates computed for each interface of each protein as the number of docking poses that presents the best AUC value for this binding site divided by the total number of poses. UNKN indicated predicted alternate interfaces with no identified alternate partners.

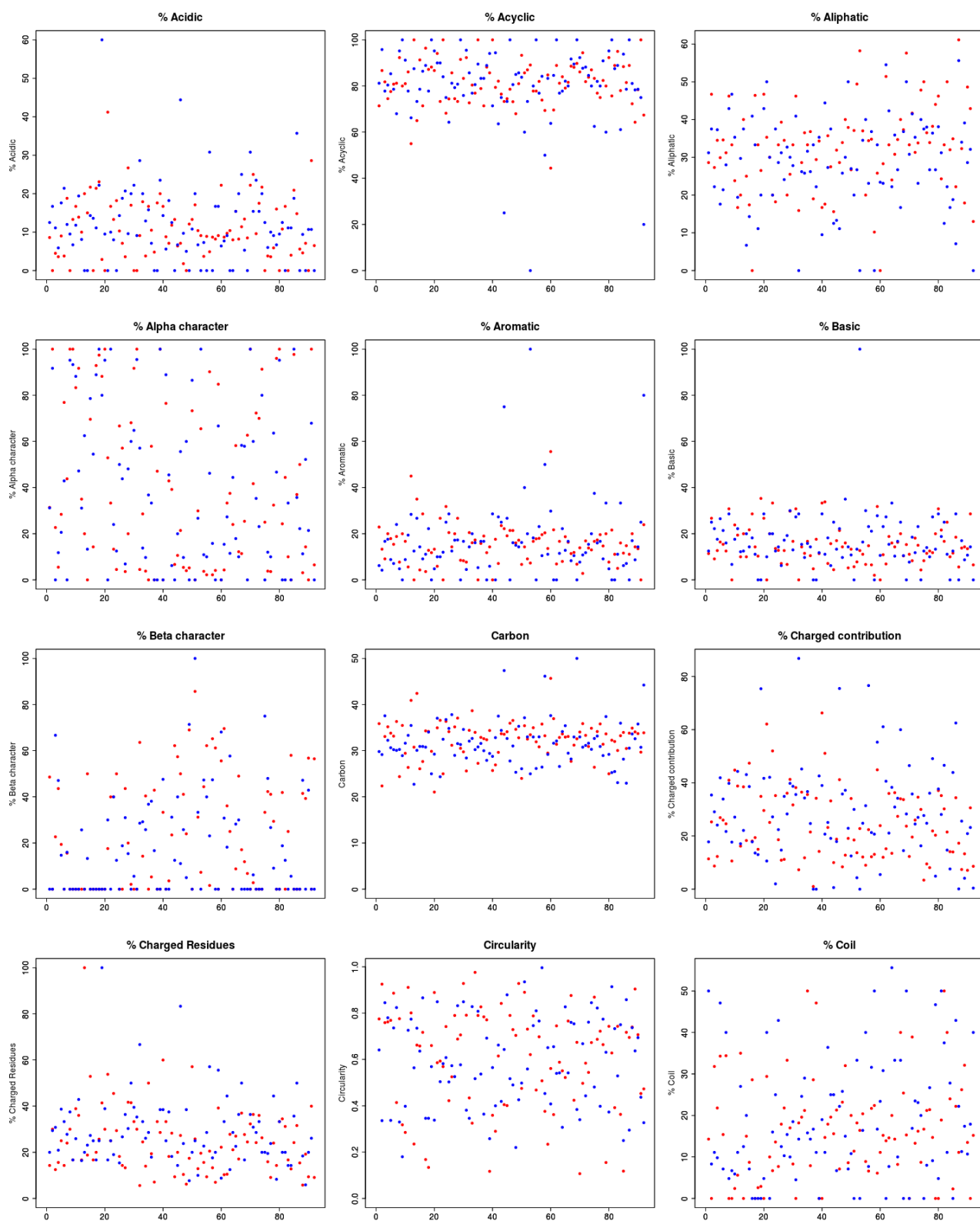


A



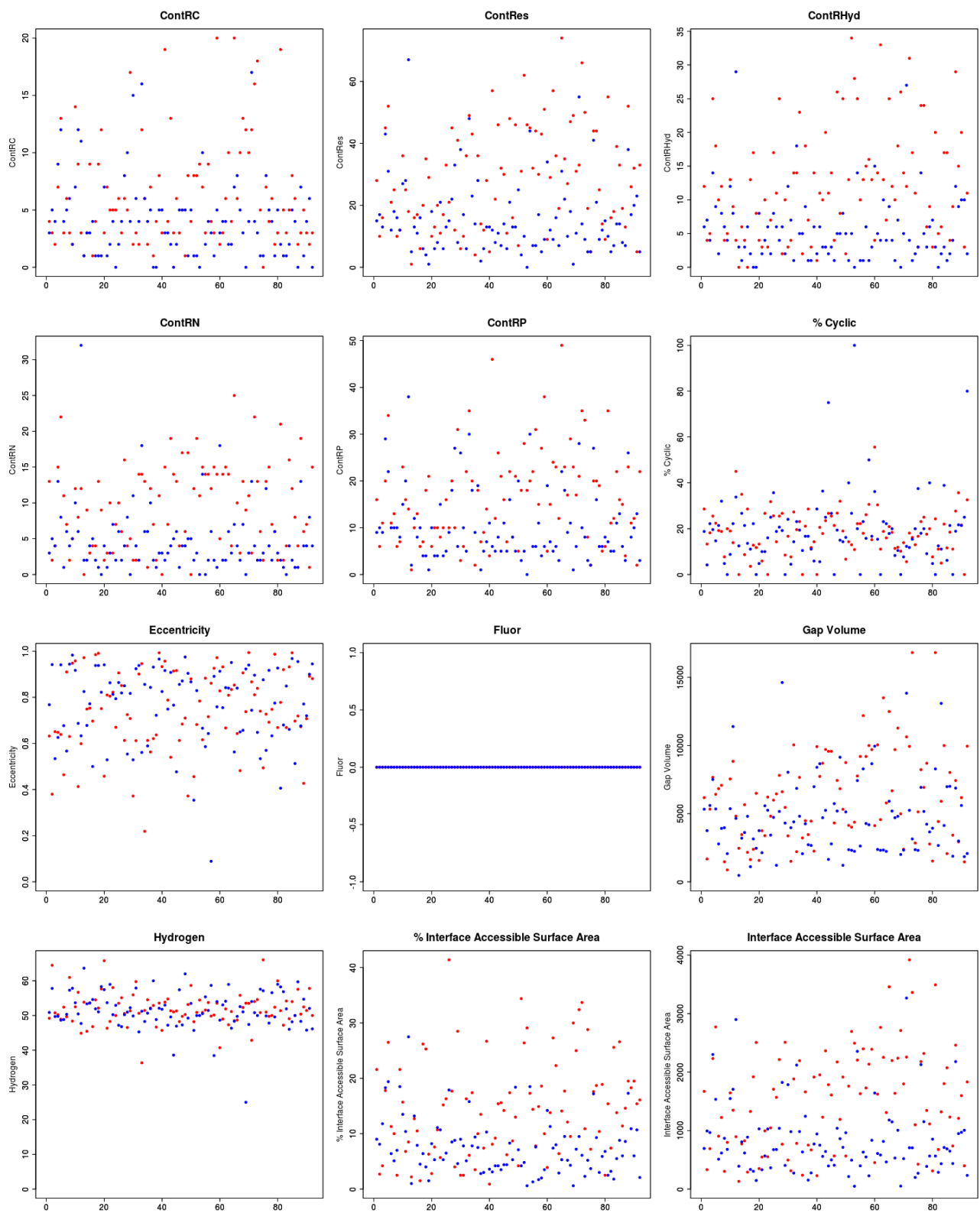
B

Figure S14 : Proteins with multiple predicted interface can present (A) one binding site predominantly targeted by the different partners during the cross-docking simulations or (B) similar occupancy rates observed between the different predicted binding sites. The PIP values are mapped on the protein's surface (high PIP residues are shown in blue and low PIP residues are shown in red) and the different partners are showed in cartoon representation in green and black.



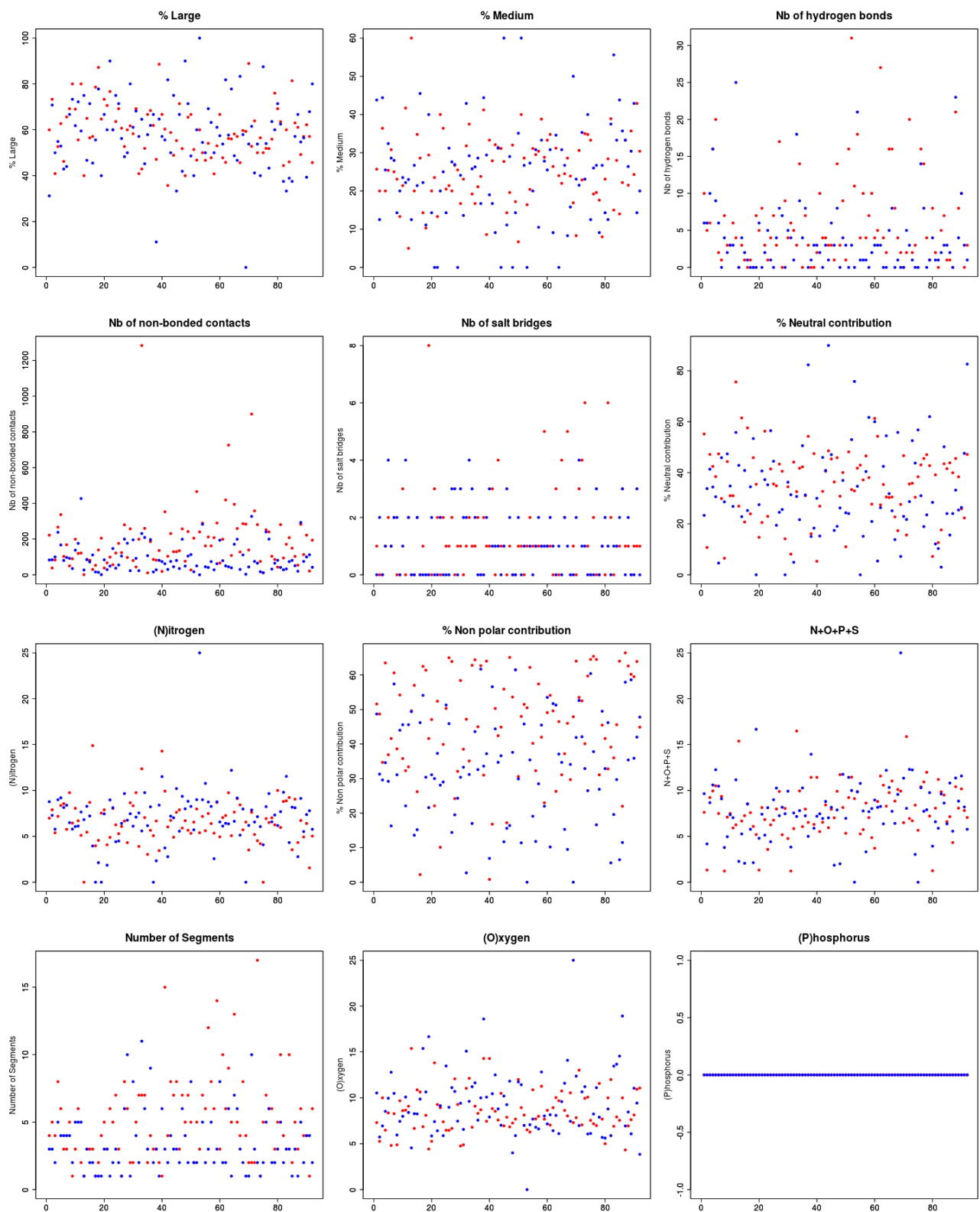
A

Figure S15 (continued next page)



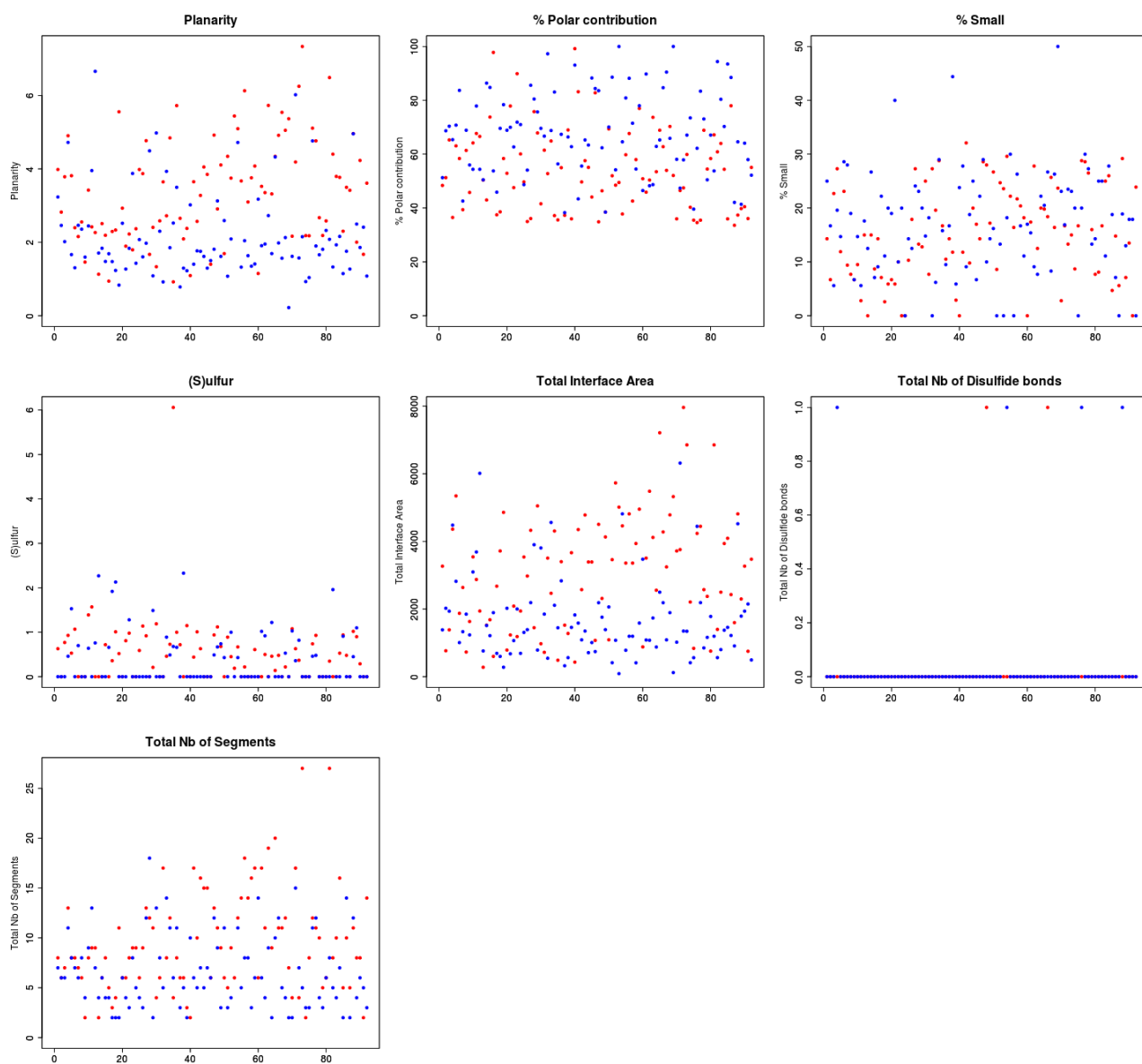
B

Figure S15 (continued next page)



C

Figure S15 (continued next page)



D

Figure S15 (A-D). Distribution of the values obtained for each of the 43 P2PI inspector descriptors with the 85 primary interface (PrimI) (showed in red) and the 85 secondary interface (SecI) (showed in blue).

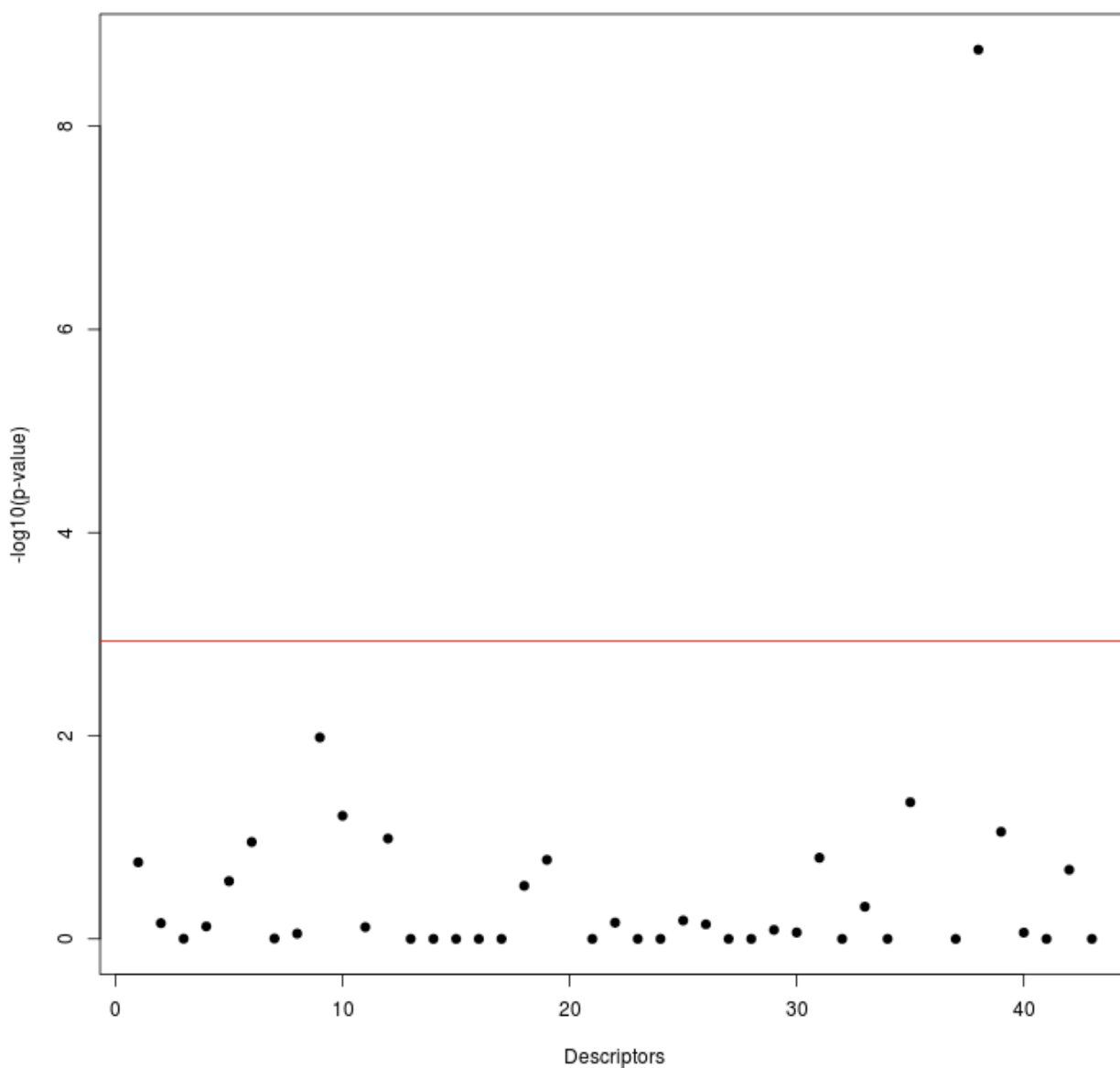


Figure S16 : The 43 P2PI inspector descriptors are plotted as the distribution of the negative logarithmic p-value ($-\log_{10}(\text{p-value})$) of the one-tailed Student test option « less ». All descriptors located above the Bonferroni threshold (red line) display a mean value significantly inferior in the PrimI than in the SecI.

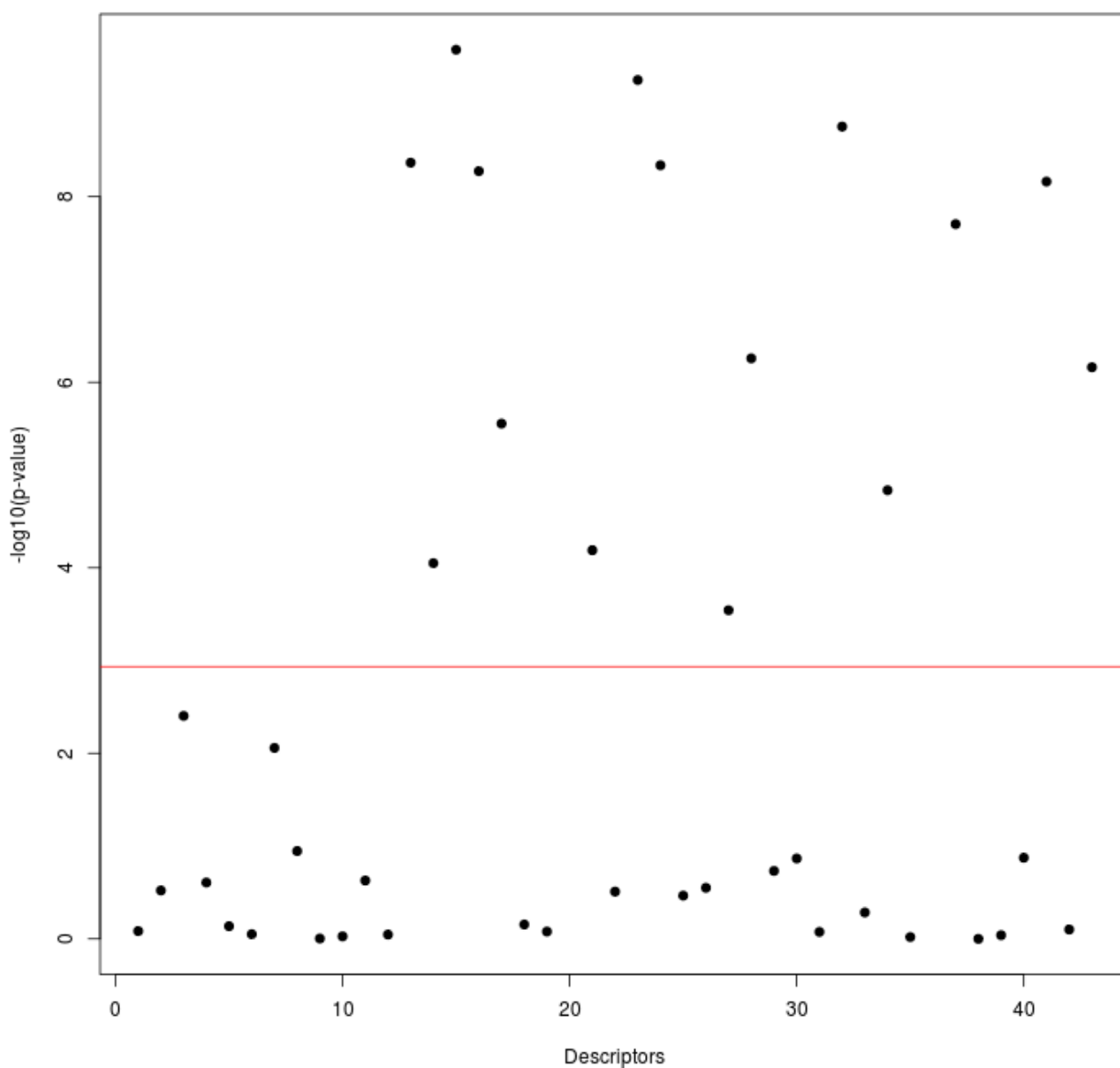


Figure S17 : The 43 P2PI inspector descriptors are plotted as the distribution of the negative logarithmic p-value ($-\log_{10}(\text{p-value})$) of the one-tailed Student test option « greater ». All descriptors located above the Bonferroni threshold (red line) display a mean value significantly superior in the PrimI than in the SecI.

PDB	Resolution	Chains	Nb residues	Couples
1AIK	2.0	C	34	1AIK_C--1AIK_N
		N	36	
1AOX	2.1	A	201	1AOX_A--1AOX_B
		B	201	
1APY	2.0	A	161	1APY_A--1APY_B
		B	141	
1ATN	2.8	A	372	1ATN_A--1ATN_D
		D	258	
1AVF	2.36	A	322	1AVF_A--1AVF_P
		P	21	
1AVO	2.8	A	60	1AVO_A--1AVO_B
		B	140	
1CK4	2.2	A	193	1CK4_A--1CK4_B
		B	195	
1D8D	2.0	A	323	1D8D_A--1D8D_B
		B	407	
1E50	2.6	A	115	1E50_A--1E50_D
		D	125	
1EF1	1.9	A	289	1EF1_A--1EF1_C
		C	87	
1EFV	2.1	A	312	1EFV_A--1EFV_B
		B	252	
1EZX	2.6	A	335	1EZX_A--1EZX_B 1EZX_A--1EZX_C
		B	36	
		C	140	
1F9E	2.9	A	153	1F9E_A--1F9E_B
		B	89	
1FNT	3.2	A	238	1FNT_A--1FNT_B 1FNT_A--1FNT_H 1FNT_B--1FNT_J 1FNT_F--1FNT_N 1FNT_H--1FNT_N
		B	247	
		F	233	
		H	196	
		J	204	
		N	233	
1GC1	2.5	C	181	1GC1_C--1GC1_G
		G	297	
1GK4	2.3	A	79	1GK4_A--1GK4_C 1GK4_A--1GK4_D 1GK4_A--1GK4_F 1GK4_C--1GK4_D 1GK4_C--1GK4_F 1GK4_D--1GK4_F
		C	70	
		D	78	
		F	74	
1GL4	2.0	A	273	1GL4_A--1GL4_B
		B	89	
1GT0	2.6	C	138	1GT0_C--1GT0_D
		D	80	

Table S1. (continued next page)

PDB	Resolution	Chains	Nb residues	Couples
1H2K	2.15	A	332	1H2K_A--1H2K_S
		S	24	
1H6V	3.0	A	490	1H6V_A--1H6V_B
		B	487	1H6V_A--1H6V_C
		C	482	1H6V_C--1H6V_E
		E	491	
1H8B	NMR	A	73	1H8B_A--1H8B_B
		B	23	
1I7X	3.0	A	522	1I7X_A--1I7X_B
		B	57	1I7X_A--1I7X_C
		C	521	
1IBC	2.73	A	167	1IBC_A--1IBC_B
		B	88	
1IW0	1.4	A	207	1IW0_A--1IW0_B
		B	209	1IW0_B--1IW0_C
		C	207	
1J1D	2.61	E	75	1J1D_E--1J1D_F
		F	116	
1JJO	3.06	A	40	1JJO_A--1JJO_C
		C	244	1JJO_A--1JJO_E
		E	33	1JJO_C--1JJO_E
1JWY	2.3	A	753	1JWY_A--1JWY_B
		B	316	
1KFU	2.5	L	699	1KFU_L--1KFU_S
		S	184	
1KU6	2.5	A	535	1KU6_A--1KU6_B
		B	61	
1LDK	3.1	A	358	1LDK_A--1LDK_B
		B	366	
1LI1	1.9	A	228	1LI1_A--1LI1_B
		B	227	1LI1_A--1LI1_C
		C	224	1LI1_B--1LI1_C
				1LI1_B--1LI1_F
		F	225	1LI1_C--1LI1_F
1LM5	1.8	A	189	1LM5_A--1LM5_B
		B	193	
1LYA	2.5	A	97	1LYA_A--1LYA_B
		B	241	

Table S1. (continued next page)

PDB	Resolution	Chains	Nb residues	Couples
1M3D	2.0	A	223	1M3D_A--1M3D_B 1M3D_A--1M3D_C
		B	224	1M3D_A--1M3D_D 1M3D_A--1M3D_E
		C	222	1M3D_B--1M3D_C 1M3D_B--1M3D_D
		D	225	1M3D_B--1M3D_E 1M3D_B--1M3D_F
		E	224	1M3D_C--1M3D_E 1M3D_C--1M3D_F
		F	223	1M3D_D--1M3D_E 1M3D_D--1M3D_F
		G	225	1M3D_D--1M3D_H 1M3D_E--1M3D_F
		H	224	1M3D_G--1M3D_H 1M3D_H--1M3D_L
1M63	2.8	C	165	1M63_C--1M63_E
		E	359	
1MDM	2.8	A	124	1MDM_A--1MDM_B
		B	129	
1MHW	1.9	A	173	1MHW_A--1MHW_C
		C	41	
1NCI	2.1	A	102	1NCI_A--1NCI_B
		B	96	
1NH2	1.9	B	46	1NH2_B--1NH2_C
		C	50	
1NME	1.6	A	146	1NME_A--1NME_B
		B	92	
1NT2	2.9	A	209	1NT2_A--1NT2_B
		B	236	
1PON	NMR	A	34	1PON_A--1PON_B
		B	34	
1PYO	1.65	A	159	1PYO_A--1PYO_B
		B	98	
1Q68	NMR	A	38	1Q68_A--1Q68_B
		B	29	
1R4M	3.0	B	418	1R4M_B--1R4M_I
		I	76	
1RF3	3.5	A	192	1RF3_A--1RF3_B
		B	24	
1RKC	2.7	A	258	1RKC_A--1RKC_B
		B	26	
1RVF	4.0	2	255	1RVF_2--1RVF_3
		3	236	1RVF_2--1RVF_4
		4	40	1RVF_3--1RVF_4
1SHW	2.2	A	138	1SHW_A--1SHW_B
		B	181	

Table S1. (continued next page)

PDB	Resolution	Chains	Nb residues	Couples
1US7	2.3	A	207	1US7_A--1US7_B
		B	194	
1VYH	3.4	A	218	1VYH_A--1VYH_C
		B	310	
1WSU	2.3	A	124	1WSU_A--1WSU_B 1WSU_C--1WSU_D
		B	122	
		C	102	
		D	121	
1Y8N	2.6	A	374	1Y8N_A--1Y8N_B
		B	97	
1YA5	2.44	A	198	1YA5_A--1YA5_T
		T	89	
1YDI	1.8	A	256	1YDI_A--1YDI_B
		B	24	
1YK1	2.9	A	394	1YK1_A--1YK1_E
		E	21	
1YY9	2.6	C	211	1YY9_C--1YY9_D
		D	220	
1ZSG	NMR	A	65	1ZSG_A--1ZSG_B
		B	22	
1ZTP	2.5	A	225	1ZTP_A--1ZTP_C
		C	218	
2AGH	NMR	A	25	2AGH_A--2AGH_B 2AGH_B--2AGH_C
		B	87	
		C	31	
2AWW	2.21	A	91	2AWW_A--2AWW_B
		B	91	
2BDN	2.53	H	217	2BDN_H--2BDN_L
		L	214	
2BKI	2.9	B	145	2BKI_B--2BKI_D
		D	78	
2BOV	2.66	A	174	2BOV_A--2BOV_B
		B	208	
2C0L	2.3	A	292	2C0L_A--2C0L_B
		B	122	
2C35	2.7	A	129	2C35_A--2C35_B
		B	171	
2C63	2.15	A	233	2C63_A--2C63_B 2C63_A--2C63_C 2C63_B--2C63_D 2C63_C--2C63_D
		B	233	
		C	233	
		D	233	
2C74	2.7	A	235	2C74_A--2C74_B
		B	234	
2C9W	1.9	A	153	2C9W_A--2C9W_C
		C	80	

Table S1 (continued next page)

PDB	Resolution	Chains	Nb residues	Couples
2D1X	1.9	A	60	2D1X_A--2D1X_B 2D1X_A--2D1X_C
		B	59	
		C	66	
2DJG	2.05	A	114	2DJG_A--2DJG_B 2DJG_A--2DJG_C 2DJG_B--2DJG_C
		B	161	
		C	68	
2DRN	NMR	A	46	2DRN_A--2DRN_C
		C	24	
2DVW	2.3	A	229	2DVW_A--2DVW_B
		B	73	
2E9W	3.5	A	468	2E9W_A--2E9W_C
		C	132	
2E9X	2.3	A	144	2E9X_A--2E9X_B 2E9X_A--2E9X_C 2E9X_A--2E9X_D 2E9X_B--2E9X_C 2E9X_B--2E9X_D 2E9X_C--2E9X_D
		B	175	
		C	186	
		D	197	
2FFK	NMR	A	242	2FFK_A--2FFK_B
		B	69	
2GD4	3.3	H	234	2GD4_H--2GD4_L
		L	54	
2GEZ	2.6	B	133	2GEZ_B--2GEZ_C
		C	166	
2GIX	2.02	A	206	2GIX_A--2GIX_B 2GIX_A--2GIX_D 2GIX_B--2GIX_D
		B	201	
		D	205	
2H0D	2.5	A	97	2H0D_A--2H0D_B
		B	100	
2I1N	1.85	A	101	2I1N_A--2I1N_B
		B	102	
2I32	2.7	A	154	2I32_A--2I32_E
		E	21	
2IAE	3.5	A	583	2IAE_A--2IAE_B
		B	376	
2JJS	1.85	A	116	2JJS_A--2JJS_C
		C	115	
2JZ3	NMR	B	118	2JZ3_B--2JZ3_C
		C	96	
2K2U	NMR	A	115	2K2U_A--2K2U_B
		B	35	
2NL9	1.55	A	140	2NL9_A--2NL9_B
		B	23	

Table S1 (continued next page)

PDB	Resolution	Chains	Nb residues	Couples
2NNA	2.1	A	182	2NNA_A--2NNA_B
		B	182	
2NNW	2.7	A	350	2NNW_A--2NNW_B
		B	227	
2NQB	2.3	D	95	2NQB_D--2NQB_G
		G	105	
2NVU	2.8	B	789	2NVU_B--2NVU_C
		C	176	
2O8A	2.61	A	295	2O8A_A--2O8A_I
		I	59	
2ODB	2.4	A	177	2ODB_A--2ODB_B
		B	35	
2OT3	2.1	A	253	2OT3_A--2OT3_B
		B	157	
2P1L	2.5	A	141	2P1L_A--2P1L_B
		B	24	
2P1M	1.8	A	90	2P1M_A--2P1M_B
		B	567	
2PAV	1.8	A	361	2PAV_A--2PAV_P
		P	139	
2PJY	3.0	A	112	2PJY_A--2PJY_B
		B	108	2PJY_A--2PJY_C
		C	79	2PJY_B--2PJY_C
2Q7N	4.0	A	480	2Q7N_A--2Q7N_B
		B	180	
2QFA	1.4	A	137	2QFA_A--2QFA_B
		B	62	2QFA_A--2QFA_C
		C	45	2QFA_B--2QFA_C
2QOU	3.93	C	206	2QOU_C--2QOU_E
		D	205	2QOU_C--2QOU_J
		E	150	2QOU_C--2QOU_N
		F	100	2QOU_D--2QOU_E
		G	150	2QOU_E--2QOU_H
		H	29	2QOU_F--2QOU_R
		I	127	2QOU_G--2QOU_I
		J	98	2QOU_G--2QOU_K
		K	11	2QOU_H--2QOU_L
		L	123	2QOU_H--2QOU_Q
		M	114	2QOU_I--2QOU_J
		N	96	2QOU_I--2QOU_N
		O	88	2QOU_J--2QOU_N
		Q	80	2QOU_K--2QOU_R
		R	55	2QOU_K--2QOU_U
S	79	2QOU_L--2QOU_Q		
U	51	2QOU_M--2QOU_S		
				2QOU_N--2QOU_S
				2QOU_O--2QOU_Q
				2QOU_R--2QOU_U

Table S1 (continued next page)

PDB	Resolution	Chains	Nb residues	Couples
2QOV	3.93	1	50	
		3	64	
		4	38	2QOV_1--2QOV_3
		D	209	2QOV_3--2QOV_L
		E	201	2QOV_4--2QOV_G
		G	176	2QOV_D--2QOV_K
		H	149	2QOV_D--2QOV_N
		K	121	2QOV_D--2QOV_P
		L	143	2QOV_E--2QOV_L
		M	136	2QOV_G--2QOV_H
		N	120	2QOV_H--2QOV_Z
		P	114	2QOV_K--2QOV_P
		T	93	2QOV_M--2QOV_V
		V	94	2QOV_T--2QOV_X
2R9P	1.4	A	24	2R9P_A--2R9P_E
		E	58	
2RGN	3.5	A	324	2RGN_A--2RGN_B 2RGN_B--2RGN_C
		B	327	
		C	177	
2RHK	1.95	A	119	2RHK_A--2RHK_C
		C	63	
2RMK	NMR	A	192	2RMK_A--2RMK_B
		B	81	
2UZI	2.0	H	114	2UZI_H--2UZI_L
		L	104	
2V17	1.65	H	222	2V17_H--2V17_L
		L	214	
2V8Q	2.1	A	102	2V8Q_A--2V8Q_B 2V8Q_A--2V8Q_E 2V8Q_B--2V8Q_E
		B	73	
		E	304	
2VGL	2.59	A	600	2VGL_A--2VGL_B 2VGL_A--2VGL_M 2VGL_A--2VGL_S 2VGL_B--2VGL_M 2VGL_B--2VGL_S 2VGL_M--2VGL_S
		B	579	
		M	396	
		S	142	
2VP7	1.65	A	66	2VP7_A--2VP7_B
		B	33	
2Z3Q	1.85	B	81	2Z3Q_B--2Z3Q_C
		C	117	
2Z5H	2.89	B	51	2Z5H_B--2Z5H_I 2Z5H_I--2Z5H_T
		I	39	
		T	34	

Table S1 (continued next page)

PDB	Resolution	Chains	Nb residues	Couples
2ZCH	2.83	H	229	2ZCH_H--2ZCH_L
		L	215	2ZCH_H--2ZCH_P
		P	237	2ZCH_L--2ZCH_P
2ZL1	2.0	A	119	2ZL1_A--2ZL1_B
		B	116	
3B6F	3.45	C	106	3B6F_C--3B6F_H
		H	99	
3BC1	1.8	B	52	3BC1_B--3BC1_E
		E	175	
3BES	2.2	L	133	3BES_L--3BES_R
		R	250	
3BJ4	2.0	A	37	3BJ4_A--3BJ4_B
		B	38	
3BPL	2.93	B	202	3BPL_B--3BPL_C
		C	194	
3BRT	2.25	B	61	3BRT_B--3BRT_C
		C	43	
3BRW	3.4	B	337	3BRW_B--3BRW_D
		D	167	
3BS5	2.0	A	83	3BS5_A--3BS5_B
		B	74	
3BT2	2.5	A	124	3BT2_A--3BT2_U
		B	40	3BT2_B--3BT2_U
		H	212	3BT2_H--3BT2_L
		L	211	3BT2_H--3BT2_U
		U	259	3BT2_L--3BT2_U
3BYH	12.0 (EM)	A	374	3BYH_A--3BYH_B
		B	231	
3C08	2.15	H	217	3C08_H--3C08_L
		L	206	
3C5J	1.8	A	178	3C5J_A--3C5J_B
		B	182	
3C66	2.6	A	529	3C66_A--3C66_C
		C	24	
3CH5	2.1	A	193	3CH5_A--3CH5_B
		B	37	
3CL3	3.2	A	172	3CL3_A--3CL3_D
		D	59	

Table S1 (continued next page)

PDB	Resolution	Chains	Nb residues	Couples
3CWB	3.51	A	443	3CWB_A--3CWB_B
		B	421	3CWB_A--3CWB_D
		D	241	3CWB_A--3CWB_E
		E	196	3CWB_A--3CWB_J
		F	100	3CWB_D--3CWB_E
		H	70	3CWB_D--3CWB_F
		J	61	3CWB_D--3CWB_H
		P	379	3CWB_D--3CWB_J
		T	79	3CWB_E--3CWB_J
3CXE	3.3	A	412	3CWB_E--3CWB_P
		B	105	3CWB_P--3CWB_T
		C	116	3CXE_A--3CXE_B
3D0G	2.8	A	597	3CXE_B--3CXE_C
		E	173	3D0G_A--3D0G_E
3D1M	1.7	A	148	
		D	99	3D1M_A--3D1M_D
3D2U	2.21	A	281	
		B	99	3D2U_A--3D2U_B
3D48	2.5	P	165	
		R	195	3D48_P--3D48_R
3D85	1.9	A	213	3D85_A--3D85_B
		B	216	3D85_A--3D85_C
		C	133	3D85_B--3D85_C
		D	290	3D85_C--3D85_D
3DGC	2.5	M	141	
		S	207	3DGC_S--3DGC_M

Table S1. List of PDB structures used to create the CC-D dataset with its corresponding resolution. The chains included in the dataset, the number of residues of each chain and the experimental partners couples are indicated in the third, fourth and fifth columns respectively.

protein	PrimI	OR (%)	SecI	OR (%)	PrimI/SecI
1AIK_C	1AIK_C--1AIK_A	69	1AIK_C--1AIK_N	31	2.2
1AOX_A	1AOX_A--homolog1V7PB1	59	1AOX_A--1AOX_B	20	2.95
1AOX_B	1AOX_B--homolog1V7PB2	68	1AOX_B--1AOX_A	7	9.71
1EF1_C	1EF1_C--1EF1_A	89	1EF1_C--1EF1_D	10	8.90
1FNT_J	1FNT_J--1FNT_I	33	1FNT_J--1FNT_B	8	4.13
1GC1_C	1GC1_C--homolog1CDH	93	1GC1_C--1GC1_G	7	13.29
1GK4_A	1GK4_A--1GK4_B	77	1GK4_A--1GK4_F	12	6.42
1GK4_C	1GK4_C--1GK4_D	85	1GK4_C--1GK4_F	13	6.54
1GK4_D	1GK4_D--1GK4_C	84	1GK4_D--1GK4_F	14	6.00
1GK4_F	1GK4_F--1GK4_E	66	1GK4_F--1GK4_D	22	3.00
1H2K_A	1H2K_A--1H2K_B	73	1H2K_A--1H2K_S	27	2.70
1I7X_A	1I7X_A--homolog1G3J	58	1I7X_A--1I7X_C	19	3.05
1JJO_A	1JJO_A--1JJO_C	70	1JJO_A--1JJO_E	22	3.18
1JJO_E	1JJO_E--1JJO_C	62	1JJO_E--1JJO_A	38	1.63
1KFU_L	1KFU_L--homolog3DF0	96	1KFU_L--1KFU_S	4	24.00
1LDK_A	1LDK_A--1LDK_E	64	1LDK_A--1LDK_B	11	5.82
1LDK_B	1LDK_B--1LDK_C	78	1LDK_B--1LDK_A	22	3.55
1LI1_A	1LI1_A--1LIA_C	73	1LI1_A--1LI1_B	22	3.32
1LI1_B	1LI1_B--1LI1_A	63	1LI1_B--1LI1_C	30	2.10
1M3D_A	1M3D_A--1M3D_C	63	1M3D_A--1M3D_B	33	1.91
1M3D_B	1M3D_B--1M3D_A	55	1M3D_B--1M3D_F	1	55.00
1M3D_C	1M3D_C--1M3D_B	49	1M3D_C--1M3D_E	1	49.00
1M3D_E	1M3D_E--1M3D_D	57	1M3D_E--1M3D_C	1	57.00
1M3D_F	1M3D_F--1M3D_D	44	1M3D_F--1M3D_B	1	44.00
1M3D_G	1M3D_G--1M3D_I	60	1M3D_G--1M3D_H	35	1.71
1M3D_L	1M3D_L--1M3D_J	44	1M3D_L--1M3D_H	1	44.00
1NH2_B	1NH2_B--1NH2_D	81	1NH2_B--1NH2_C	19	4.26
1NH2_C	1NH2_C--1NH2_D	44	1NH2_C--1NH2_B	16	2.75
1PYO_B	1PYO_B--1PYO_A	88	1PYO_B--1PYO_D	6	14.67
1R4M_B	1R4M_B--1R4M_A	60	1R4M_B--1R4M_I	20	3.00
1R4M_I	1R4M_I--1R4M_B	100	1R4M_I--1R4M_A	0	NA
1RF3_A	1RF3_A--1RF3_E	44	1RF3_A--1RF3_B	26	1.69
1VYH_A	1VYH_A--1VYH_B	72	1VYH_A--1VYH_C	13	5.54
1YY9_C	1YY9_C--1YY9_D	98	1YY9_C--1YY9_A	2	49.00
1YY9_D	1YY9_D--1YY9_C	62	1YY9_D--1YY9_A	38	1.63
2BDN_H	2BDN_H--2BDN_L	64	2BDN_H--2BDN_A	36	1.78
2BDN_L	2BDN_L--2BDN_H	92	2BDN_L--2BDN_A	8	11.5
2BKI_B	2BKI_B--2BKI_A	63	2BKI_B--2BKI_D	37	1.70
2BKI_D	2BKI_D--2BKI_B	63	2BKI_D--2BKI_A	37	1.70
2BOV_A	2BOV_A--homolg1UAD	79	2BOV_A--2BOV_B	21	3.76
2COL_A	2COL_A--homolog1FCH	80	2COL_A--2COL_B	20	4.00
2C74_A	2C74_A--2C74_P	81	2C74_A--2C74_B	19	4.26
2C74_B	2C74_B--2C74_Q	74	2C74_B--2C74_A	26	2.85
2C9W_C	2C9W_C--2C9W_B	77	2C9W_C--2C9W_A	23	3.35

Table S2 (continued next page)

protein	PrimI	OR (%)	SecI	OR (%)	PrimI/SecI
2DJG_A	2DJG_A--2DJG_B	78	2DJG_A--2DJG_C	22	3.55
2DJG_B	2DJG_B--2DJG_A	71	2DJG_B--2DJG_C	29	2.45
2DRN_A	2DRN_A--2DRN_B	72	2DRN_A--2DRN_C	28	2.57
2E9W_A	2E9W_A--2E9W_B	92	2E9W_A--2E9W_C	8	11.50
2E9X_A	2E9X_A--2E9X_D	62	2E9X_A--2E9X_F	9	6.89
2E9X_C	2E9X_C--2E9X_A	58	2E9X_C--2E9X_B	16	3.63
2GEZ_B	2GEZ_B--2GEZ_A	71	2GEZ_B--2GEZ_C	13	5.46
2GEZ_C	2GEZ_C--2GEZ_D	46	2GEZ_C--2GEZ_B	5	9.20
2NNW_A	2NNW_A--homolog3NMU	84	2NNW_A--2NNW_B	5	16.80
2NQB_G	2NQB_G--2NQB_H	71	2NQB_G--2NQB_D	9	7.89
2O8A_I	2O8A_I--homolog3N5U	83	2O8A_I--2O8A_A	17	4.88
2P1L_B	2P1L_B--homologH	64	2P1L_B--2P1L_A	36	1.78
2PJY_C	2PJY_C--2PJY_D	57	2PJY_C--2PJY_A	22	2.59
2RGN_B	2RGN_B--2RGN_C	68	2RGN_B--2RGN_A	32	2.13
2RHK_A	2RHK_A--2RHK_B	73	2RHK_A--2RHK_C	27	2.70
2UZI_H	2UZI_H--2UZI_L	84	2UZI_H--2UZI_R	16	5.25
2UZI_L	2UZI_L--2UZI_H	75	2UZI_L--2UZI_R	25	3.00
2V8Q_A	2V8Q_A--2V8Q_B	80	2V8Q_A--2V8Q_E	20	4.00
2V8Q_E	2V8Q_E--2V8Q_A	74	2V8Q_E--2V8Q_B	26	2.85
2VGL_B	2VGL_B--2VGL_M	58	2VGL_B--2VGL_S	7	8.29
2VGL_M	2VGL_M--2VGL_B	76	2VGL_M--2VGL_S	16	4.75
2VGL_S	2VGL_S--2VGL_A	67	2VGL_S--2VGL_B	18	3.72
2Z3Q_C	2Z3Q_C--2Z3Q_D	62	2Z3Q_C--2Z3Q_B	38	1.63
2Z5H_B	2Z5H_B--2Z5H_A	48	2Z5H_B--2Z5H_I	13	3.69
2ZCH_H	2ZCH_H--2ZCH_L	83	2ZCH_H--2ZCH_P	17	4.88
2ZCH_L	2ZCH_L--2ZCH_H	89	2ZCH_L--2ZCH_P	11	8.09
3B6F_C	3B6F_C--3B6F_D	68	3B6F_C--3B6F_E	12	5.67
3BC1_E	3BC1_E--3BC1_F	64	3BC1_E--3BC1_B	9	7.11
3BES_L	3BES_L--3BES_A	56	3BES_L--3BES_R	27	2.07
3BES_R	3BES_R--3BES_D	31	3BES_R--3BES_L	7	4.43
3BT2_H	3BT2_H--3BT2_U	68	3BT2_H--3BT2_L	32	2.13
3BT2_L	3BT2_L--3BT2_H	70	3BT2_L--3BT2_U	30	2.33
3CH5_A	3CH5_A--homolog_1IBR	73	3CH5_A--3CH5_B	27	2.70
3CL3_D	3CL3_D--3CL3_B	68	3CL3_D--3CL3_A	13	5.23
3CWB_B	3CWB_B--3CWB_O	86	3CWB_B--3CWB_A	3	28.67
3CWB_E	3CWB_E--3CWB_P	66	3CWB_E--3CWB_D	7	9.43
3CWB_F	3CWB_F--3CWB_C	68	3CWB_F--3CWB_D	15	4.53
3D85_A	3D85_A--3D85_B	96	3D85_A--3D85_C	4	24.00
3D85_B	3D85_B--3D85_A	67	3D85_B--3D85_C	33	2.03
3D85_C	3D85_C--3D85_D	58	3D85_C--3D85_B	10	5.80
3DGC_M	3DGC_M--3DGC_S	70	3DGC_M--3DGC_R	30	2.33

Table S2. List of proteins presenting occupancy rates (OR) at least 50% superior for the Primary Interface (PrimI) compared to Secondary Interface (SecI). The last column PrimI/SecI indicates the ratio value of the PrimI's occupancy rate over the SecI's occupancy rate.

Descriptors	Greater	Less
% Acidic	7.21E-01	2.79E-01
% Acyclic	3.43E-01	6.57E-01
% Aliphatic	1.44E-02	9.86E-01
% Alpha character	2.55E-01	7.45E-01
% Aromatic	6.97E-01	3.03E-01
% Basic	8.89E-01	1.11E-01
% Beta character	1.38E-02	9.86E-01
Carbon	1.24E-02	9.88E-01
% Charged contribution	9.81E-01	1.95E-02
% Charged Residues	8.55E-01	1.45E-01
Circularity	2.70E-01	7.30E-01
% Coil	8.34E-01	1.66E-01
ContRes	1.09E-04	1.00E+00
ContRC	1.61E-08	1.00E+00
ContRHyd	8.74E-10	1.00E+00
ContRN	2.54E-08	1.00E+00
ContRP	8.18E-06	1.00E+00
% Cyclic	6.57E-01	3.43E-01
Eccentricity	7.87E-01	2.13E-01
Fluor	NA	NA
Gap Volume	6.30E-05	1.00E+00
Hydrogen	5.91E-01	4.09E-01
% Interface Accessible Surface Area	1.71E-09	1.00E+00
Interface Accessible Surface Area	1.03E-08	1.00E+00
% Large	4.23E-01	5.77E-01
% Medium	2.29E-01	7.71E-01
Nb of hydrogen bonds	1.09E-03	9.99E-01
Nb of non-bonded contacts	1.55E-06	1.00E+00
Nb of salt bridges	1.61E-01	8.39E-01
% Neutral contribution	9.19E-02	9.08E-01
(N)itrogen	9.37E-01	6.30E-02
% Non polar contribution	2.60E-08	1.00E+00
N+O+P+S	3.13E-01	6.87E-01
Number of Segments	8.66E-05	1.00E+00
(O)xygen	9.26E-01	7.44E-02
(P)hosphorus	NA	NA
Planarity	1.61E-07	1.00E+00
% Polar contribution	1.00E+00	2.61E-08
% Small	8.96E-01	1.04E-01
(S)ulfur	1.86E-01	8.14E-01
Total Interface Area	1.88E-08	1.00E+00
Total Nb of Disulfide bonds	7.91E-01	2.09E-01
Total Nb of Segments	3.25E-06	1.00E+00

Table S3. p-values obtained for each one of the 43 2P2I inspector descriptors in the one-tailed Student test with the option « greater » (column « Greater ») and « less » (column « Less »). The significant p-values using the Bonferonni threshold are indicated in bold.